Online gas and particle phase measurements of organosulfates, organosulfonates and nitrooxyorganosulfates in Beijing utilizing a FIGAERO ToF-CIMS

Michael Le Breton[1], Yujue Wang[2], Åsa M Hallquist[3], Ravi Kant Pathak[1], Jing Zheng[2], Yudong Yang[2], Dongjie Shang[2], Marianne Glasius[4], Thomas J Bannan[5], Qianyun Liu[6], Chak. K. Chan[7], Carl. J. Percival[8], Wenfei Zhu[9,] Shengrong Lou[9], David Topping[5], Yuchen Wang[6], Jianzhen Yu[6], Keding Lu[2], Song Guo[2], Min Hu[2] and Mattias Hallquist[1]

[1] Department of Chemistry and Molecular Biology, University of Gothenburg, Gothenburg, Sweden
[2] State Key Joint Laboratory of Environmental Simulation and Pollution Control, College of Environmental Sciences and Engineering, Peking University, Beijing, China
[3] IVL Swedish Environmental Research Institute, Gothenburg, Sweden
[4] Department of Chemistry and iNANO, Aarhus University, 8000 Aarhus C, Denmark
[5] Centre for Atmospheric Science, School of Earth, Atmospheric and Environmental Science, University of Manchester, Manchester, UK
[6] Division of Environment and Sustainability, The Hong Kong University of Science and Technology, Clearwater Bay, Kowloon, Hong Kong
[7] (School of Energy and Environment, City University of Hong Kong, Hong Kong
[8] Jet Propulsion laboratory, Pasadena, California, USA.
[9] Shanghai Academy of Environmental Sciences, Shanghai 200233, China

Correspondence to: M. Le Breton (Michael.le.breton@gu.se) and S. Guo (guosong@pku.edu.cn)

Abstract. A Time of Flight Chemical Ionisation Mass spectrometer (CIMS) utilizing the Filter Inlet for Gas and AEROsol (FIGAERO) was deployed at a regional site 40 km north west of Beijing and successfully identified and measured 17 sulfur containing organics (SCOs = organo/nitrooxyorgano sulfates and sulfonates) with biogenic and anthropogenic precursors. The SCOs were quantified using laboratory synthesized standards of lactic acid sulfate and nitrophenol organosulfate (NP OS): The variation in field observations were confirmed by comparison to offline measurement techniques (orbitrap and HPLC) using daily averages. The mean total (of the 17 identified by CIMS) SCO particle mass concentration was 210 ± 110 ng m^{-3} and had a maxima of 540 ng m^{-3}, although contributed to only $2 \pm 1\%$ of the organic aerosol (OA). The CIMS identified a persistent gas phase presence of SCOs in the ambient air, which was further supported by separate vapour pressure measurements of NP OS by a Knudsen Effusions Mass Spectrometer (KEMS). An increase in RH promoted partitioning of SCO to the particle phase whereas higher temperatures favored higher gas phase concentrations.

Biogenic emissions contributed to only 19% of total SCOs analysed in this study. Here $C_{10}H_{16}NSO_7$, a monoterpene derived SCO, representing the highest fraction (10%) followed by an isoprene-derived SCO. The Anthropogenic SCOs with PAH and aromatic precursors dominated the SCO mass loading (51%) with $C_{11}H_{11}SO_7$, derived from methyl

napthalene oxidation, contributing to 40 ng m^{-3} and 0.3% of the OA mass. Anthropogenic related SCOs correlated well with benzene, although their abundance depended highly on the photochemical age of the air mass, tracked using the ratio between pinonic acid and its oxidation product, acting as a qualitative photochemical clock. In addition to typical anthropogenic and biogenic precursor the biomass burning precursor nitrophenol (NP) provided significant level of NP OS. It must be noted that the contribution analysis here is only representative of the SCOs detected, where there are likely to be many more SCOs present which the CIMS has not identified.

Gas and particle phase measurements of glycolic acid suggest that partitioning towards the particle phase promotes glycolic acid sulfate production, contrary to the current formation mechanism suggested in the literature. Furthermore, the $HSO_4.H_2SO_4^-$ cluster measured by the CIMS was utilized as a qualitative marker for acidity and indicates that the production of total SCOs is efficient in highly acidic aerosols with high SO_4^{2-} and organic content. This dependency becomes more complex when observing individual SCOs due to variability of specific VOC precursors.

1. Introduction

Atmospheric particulate matter (PM) is known to play a major role in affecting climate and air quality leading to severe health issues, such as respiratory and cardiovascular degradation (Pope *et al.*, 2002; 2011; Kim *et al*., 2015). Secondary organic aerosols (SOA), formed through reactions of volatile organic compounds (VOCs) yielding semi volatile products that partition into the aerosol phase, represents a significant fraction of PM (Hallquist *et al*., 2009) and remains the most poorly understood PM source (Foley *et al*., 2010) due to the complexity of its chemical nature, resulting in discrepancies between observations and models (Heald *et al*., 2005). Annual average PM_1 (particulate matter of diameter less than 1 micron) concentrations in Beijing reached 89.5 µg m^{-3} in 2013 and, although recently dropped to 80.6 µg m^3, is still significantly above the Chinese National Ambient air quality Standard (CNAAQS, 35 µg m^3 annual average). The knowledge gap of PM primary emissions and secondary production limits scientifically based abatement strategies targeting effects of secondary pollution in highly polluted regions (Hallquist *et al.*, 2016; Zhang *et al.,* 2012a). Therefore, Beijing is an ideal case study region for intense measurement campaigns to increase our understanding of the sources and processes involved in atmospheric aerosol chemistry in megacities. A growing number of field studies in this region have been performed in recent years, specifically focused on the haze events investigating the composition of primary and secondary particle aerosols and their formation mechanisms (Guo *et al.,* 2012, 2014, 2013; Huang *et al*., 2010; Hu *et al.,* 2016, 2017; Li *et al.,* 2017).

Organosulfates (OSs), here part of sulfur containing organics (SCOs), are known important SOA components formed by reactions between reactive organic compounds and sulfate (Iinuma *et al.,* 2007; Surratt *et al*., 2007, 2008), which is generated by the oxidation of SO_2, primarily emitted by fossil fuel combustion (Wuebbles and Jain, 2001). OSs have previously been measured in ambient aerosols at a number of geographical locations, from remote regions to highly populated urban environments (Surratt *et al*., 2007, 2008; Kristensen *et al.,* 2011; Stone *et al*., 2012; Zhang *et al*.,

2012b; Worton *et al*., 2013; Shalamzari *et al*., 2013; Hansen *et al*., 2014) although their composition and contribution to organic mass can vary significantly (Huang *et al*., 2015). To date, several of their precursors are not known (e.g. Hansen *et al*., 2014). Mechanistic studies reveal multiple possible pathways for SCO formation, which depend on availability of reactants in the atmosphere (Hettiyadura *et al*., 2015), increasing the complexity of understanding their occurrence and descriptions within models. Measurements of specific SCOs have shown they may individually contribute up to 1% of the total organics (Olson *et al*., 2011; Liao *et al.,* 2015).

Isoprene SCOs are hypothesized to be the most abundant precursor in the ambient atmosphere (Surratt *et al*., 2007; Liao *et al.,* 2015) and are often used as markers of isoprene-derived SOA in field campaigns (Zhang *et al*., 2012b). Aromatic SCOs, considered to originate from anthropogenic sources, have been recently observed in Lahore, Pakistan (Stone *et al*., 2012) and in urban sites in East Asia (Lin *et al*., 2012). Riva *et al*. (2015 and 2016) have also previously probed the SCO formation potential from PAH and alkane oxidation in the presence of acidic sulfate aerosols. Glycolic acid sulfate (GAS) is considered another potentially important SCO due to its common abundance and possible sources (Olson *et al*., 2011; Liao *et al*., 2015). It is thought to form via a gas phase precursor reaction with an acidic aerosol sulfate or from the particle phase reaction of methyl vinyl ketone with a sulfate particle, although both of these mechanisms are yet to be proven (Liao *et al*., 2015). GAS is also the only SCO to date, which has been detected in the gas phase (Ehn *et al*., 2010), providing possible importance of gas to particle phase partitioning of some SCOs.

SCOs are thought to be good tracers for heterogeneous aerosol phase chemistry and SOA formation since the known formation mechanisms involve reactive uptake of gas phase organic species onto aerosol (Surratt *et al.,* 2010). Due to their hydrophilic nature, polarity and relatively low volatility, they may significantly help nanoparticle growth and increase their potential to become cloud condensation nuclei (Smith *et al*., 2008). Therefore, it is imperative to improve our knowledge of SCO abundance, formation, distribution, precursors and fate to help develop our understanding of SOA formation.

Mass spectrometry coupled with electrospray ionization is a common method to detect SCOs (Iinuma *et al*., 2007; Reemtsma *et al*., 2006; Surratt *et al*., 2007; Gomez-Gonzalez *et al*., 2008). Liquid chromatography can efficiently separate aromatic and monoterpene derived organic sulfates containing aromatic rings or long alkyl chains and is used for speciation of SCOs (Stone *et al*., 2012). Furthermore, hydrophilic interaction liquid chromatography has been utilized as a very selective technique due to its ability to allow the SCO to retain a carboxyl group, enabling detection of a larger suite of compounds (Gao *et al.,* 2006). The methods above often rely on sampling filters taken in the field and therefore provide a relatively low measurement frequency. This can limit the ability to evaluate production pathways when concentrations are often integrated over a period of hours or more. Further reactions on filters between the organics and sulfates has also been postulated to add a bias to the SCO concentration measured with respect to initial deposition onto the filter (Hettiyadura *et al*., 2017; Kristensen *et al*., 2016). Recently, a Particle Analysis Laser Mass Spectrometer (PALMS) was utilized to measure a number of OSs over the United States highlighting the ability of time of flight mass spectrometers to measure several SCOs at high time frequencies (Liao *et al*., 2015).

This study utilizes a Filter Inlet for Gas and AEROsol (FIGAERO) Time of Flight Chemical Ionisation Mass Spectrometer (ToF-CIMS) for the measurement of ambient SCOs at a semi-rural site 40 km from Beijing, China. This instrument enables measurements of either the gas-phase components or thermally desorbed particles by a high resolution mass spectrometer via a multi-port inlet, as described in detail by Lopez-Hilfiker *et al.,* (2014). The soft and selective ionization technique and high time resolution coupled with the FIGAERO enables the simultaneous detection and measurement of SCOs in the gas and particle phase at ng m^{-3} concentrations. This work aims to identify dominant SCOs in Beijing and their precursors. The high time resolution measurements are utilized to probe their abundance under different chemical and environmental regimes providing insight into their formation.

2. Experimental

2.1 Site description

The data presented here was collected during the measurement campaign "Photochemical smog in China" with an initiative to enhance our understanding of SOA formation via photochemical smog in China (Hallquist *et al.*, 2016). The campaign was coordinated by Peking University (PKU) and University of Gothenburg with focus on spring/summertime episodic pollution episodes in Northeast China through gas and particle phase measurements. The setup was situated at a semi-rural site 40 km North East of downtown Beijing close to Changping town (40.2207° N, 116.2312° E). All on-line instruments sampled from inlets on the 4th floor laboratory (12 metres above ground) at Peking University Changping Campus from the 13th May to 23rd June 2016, while filter measurements took place on the roof. The average temperature and humidity throughout the campaign were 23°C and 44% respectively. The wind speed averaged at 2 ms^{-1} from the South-South West. A total of 4 pollution episodes were observed during the campaign period, which are classified as sustained periods of high aerosol loading reaching a maximum of 115 micrograms per cubic meter (µg m^{-3}). The episodes were dominated by organic and nitrate aerosols although episode 3 contained high sulfate loading, equal to that of nitrate. The mass loading for the semi-rural site showed good correlation with the PKU campus measurement site (30 km South-South-West of the Changping site and 12 km North West of downtown Beijing) throughout the campaign allowing for extrapolation of the semi-rural site results to inner city conditions. HYSPLIT back trajectory results showed the pollution episodes often correlated with air masses coming from the direction of Beijing (South-South-East). Clean air days were mostly North Westerly winds with clean air coming from the rural mountain regions North West of Beijing and the measurement site.

A high resolution Time of Flight Aerosol Mass Spectrometer (ToF-AMS) was utilized to measure the mass concentrations and size distributions of non-refractory species in submicron aerosols, including organics, sulfate, ammonium and chloride (DeCarlo *et al., 2006*; Hu *et al.,* 2013). The setup of this instrument has been previously

described by Hu *et al.* (2016). An Ionicon Analytik high sensitivity PTR-MS (Proton TRansfer Mass Spectrometer) as described by de Gouw and Warneke *et al.*, (2007) provided supporting precursor VOC measurements.

2.3 ToF-CIMS setup

Gas and particle phase species were measured using an iodide ToF-CIMS coupled to the FIGAERO inlet (Lopez-Hilfiker *et al.*, 2014). The ToF-CIMS can be operated in either negative or positive ionization modes, and a variety of reagent ion sources can be used. In this work the ToF-CIMS was operated in single reflection mode. The negative Iodide ion (I^-) was used as the reagent in all experiments. Dry UHP N_2 was passed over a permeation tube containing liquid CH_3I (Alfa Aesar, 99%), and the flow was passing a Tofwerk X-Ray Ion Source type P (operated at 9.5 kV and 150 μA) to produce the ionization ions. The ionized gas was then directed to the IMR through an orifice (Ø = 1 μm). Reaction products (e.g., compound X) were identified by their corresponding cluster ions, XI^- or the deprotonated ion, allowing for the collection of whole-molecule data. The nominal reagent and sample flow rates into the Ion-Molecule Reaction (IMR) chamber of the instrument were 3.5 liters per minute (LPM) and 2 LPM respectively. The IMR itself was temperature controlled at 40˚C and operated at a nominal pressure of 500 mbar. The ToF-CIMS was configured to measure singularly charged ions with a mass to charge ratio (*m/z*) of 7 – 620, a reduced mass range in order to compensate for the lower count rate emitted by the soft X-ray source with respect to the Polonium-235 radioactive source as commonly deployed. The tuning was optimized to increase sensitivity, which resulted in a spectral resolution of 3500. The mass range was at some instances during the campaign changed to a higher mass range (1000 *m/z*) to ensure no major contributing peaks were being unaccounted for. Perfluoropentanoic acid was utilised as a mass calibrant up to *m/z* 527 through its dimer and trimer. This range of mass calibration peaks also limited accurate peak identification above *m/z* 620.

2.4 FIGAERO inlet

The FIGAERO inlet collected particles on a Zefluor® PTFE membrane filter. The aerosol sample line was composed of 12 mm copper tubing, while 12 mm Teflon tubing was used for the gas sample line. The FIGAERO was operated in a cyclic pattern; 25 minute of gas phase sampling and simultaneous particle collection, followed by a 20 minute period during which the filter was shifted into positioned over the IMR inlet and the collected particle mass was desorbed. Desorption was facilitated by a 2 LPM flow of heated UHP N_2 over the filter. The temperature of the N_2 was increased from 20 to 250˚C in 15 minutes (3.5˚C min^{-1}), followed by a 5 minute temperature soak time to ensure that all remaining mass that volatilizes at 250˚C was removed from the filter. The resulting desorption time series profiles allowed for a distinct separation of measured species as a function of their thermal properties.

2.5 SCO Measurement

2.5.1 Identification

Spectral analysis was performed using Towfware V2.5.11. the average peak shape for the tuning utilised for this campaign was used to calculate the mass resolution and optimization of the baseline fit. The mass spectrum was mass calibrated (allowing for accurate centroid peak position to be estimated, improving on a Gaussian assumption) using 4 ions up to mass 527 (the dimer of perfluorpentanoic acid) and applying a custom peak shape to achieve accurately peak identification below 5 ppm error across the mass range (0-620 AMU). A time series of the mass calibrant error for the entire campaign (figure SI1) illustrates how the error deviated by only +/-1 throughout the measurement period. This provides confidence that variation in signal and peak positioning did not result in large errors of identification and quantification of the analyzed peaks. *A priori* unknown peaks were added to resolve overlapping peaks on the spectra until the residual was less than 5%. Each unknown peak was assigned a chemical formula using the peaks exact mass maxima to 5 decimal places and also isotopic ratios of subsequent minor peaks. An accurate fitting was characterized by a ppm error of less than 5 and subsequent accurate fitting of isotopic peaks. An example of the spectra and peak fitting can be found in Figure 1, highlighting the mass spectral fit for GAS and $C_9H_9SO_5$.. Although the structure cannot be determined with CIMS, it is assumed that no fragmentation of larger SCO species contribute to the SCO identified due to the soft ionization technique employed. The SCOs were identified in the spectra as negative ions assumed to be formed by hydrogen removal. Here, we present 17 SCOs that were identified in the mass spectra, which are displayed in Table 1 with their respective exact mass, formula, literature nomenclature and possible precursors. The peak fittings for all 17 SCOs is presented in the supplementary (SI2). All 17 SCOs represented a significant signal in the average desorption spectra from the particle phase analysis. It must be noted that gas phase spectra at times contained other ions at a similar mass to the SCOs that contributed to higher counts than the SCO. This may result in a variable error to the measurement, although this should be at a minimum due to the use of a custom peak shape and low general mass calibration error of the spectra. The SCOs detected ions ranged from 154.96 *m/z* (GAS) to 294.06 *m/z* ($C_{10}H_{11}NSO_7$). The number of oxygen in the SCO ranged from O_3 ($C_7H_7SO_3$) to O_7 ($C_5H_8SO_7$). It is acknowledged that the CIMS may not detect all SCOs in the ambient air due to peak fitting resolution limitations and limits of detection, therefore enabling the possibility for misrepresentation of the dominant SCO and an underestimation of total abundance. However, no physical features of the SCO (structure, O:C ratio, mass etc.) should inhibit the CIMS identifying the major SCO in the Beijing ambient air. Consequently, we here, and to facilitate descriptions of the relationship between individual SCOs and the total SCO measure, assumed that the measured SCOs do represent a significant fraction.

2.5.2 Quantification of SCOs

The OS and NOS calibrations normalized to formic acid calibrations (as described in le Breton *et al*., 2012, 2013) to account for any drift in sensitivity throughout the campaign. This relative sensitivity technique has been previously utilized for N_2O_5 and $ClNO_2$ and has been verified with laboratory experiments (Le Breton *et al*., 2014). As a result of low mass range of the SCOs, common functionality, relatively small change in polarity and lack of available stable SCO standards, we calibrated for 2 SCOs (lactic acid sulfate (LAS) and NP OS) and applied an average sensitivity for all the SCOs detected in Beijing. The ToF-CIMS sensitivity utilizing iodide as a reagent ion is known to vary by up to 3 orders of magnitude; therefore, further work is necessary to develop SCO standards and assess possible variations in sensitivity. NP OS is available commercially from Sigma Aldrich and was utilised to calibrate for the NOS's. L(+) Lactic acid from Sigma Aldrich (95%) was utilised as the preliminary agent for lactic acid sulfate synthesis and was produced using the same technique as Olson *et al*. (2011). Briefly, a solution of 76.1 mg, 1.29 mmol, lactic acid in 2 mL di-methyl-formamide (DMF) was added dropwise to sulphur trioxide pyridine (0.96g, 7.75mmol) in 2mL DMF at 0 °C. The solution is then stirred for 1 hour at 0 °C and 40 minutes at room temperature, the solution is re-cooled to 0 °C and trimethylamine (0.23 mL, 1.66 mmol) was added for quenching and the mixture wad further stirred for 1 hour. The solvent is then evaporated under vacuum and NMR is directly utilised to calculate the purity which was found to be 8.2%.

A known mass of the solid calibrant (NP OS and Lactic acid sulfate) was added to 3 different volumes of milliQ water to produce different concentration standards. A known volume of each solution was then placed onto the FIGAERO filter and a desorption cycle was performed. The total ion counts for the HR SCO peak relates directly to the sensitivity of the system with respect to total ion counts per molecule reaching the detector. Figure 2 shows a 3-point calibration curve for NP OS and the corresponding thermogram, mass spectra and peak fit. The sensitivity of LAS and NP OS calibrations were calculated to be 2.0 and 1.6 ion counts per ppt Hz^{-1} respectively. All SCO were calibrated using the LAS sensitivity and all NOS using the NP OS sensitivity.

During desorption of both SCOs, fragmentation of the organic core and sulphate group was observed resulting in a desorption profile at *m/z* 97 (the bisulphate ion) and the deprotonated organic mass, i.e. $C_3H_5O_3$ for lactic acid. A number of different temperature ramping rates were performed with the FIGAERO to further probe the fragmentation and highlighted an increase in ramp rate (°C/minute) decreased the calculated sensitivity due to an increase in fragmentation. This not only serves to highlight how the calibration tests of a species must mimic the exact measurement conditions, but also suggests potential interferences from fragmentation on the organic *m/z*´s. The relatively low concentration of the organic precursor with respect to the SCO results in little error in quantification, although this ratio may significantly change in different air masses and a number of products of organic oxidation may fragment resulting in a significant error. This fragmentation can also be observed within the high resolution thermograms of the FIGAERO as a double desorption and further highlights the necessity for detailed thermogram analysis to accurately deconvolve desorption's relevant only to particle loss from the filter and not fragmentation or ion chemistry in the IMR. The fragmentation is considered to be constant throughout the campaign. The error for the SCO measurements may vary

for each individual SCO possibly due to structure, volatility and fragmentation. It is commonly accepted within the literature for compounds lacking calibration that a functional group sensitivity can be applied (e.g. Lee *et al*., (2016) for ONs). Here we calculate an average error of 52 % for the SCOs, calculated using the standard deviation of the NP OS calibration time series data.

5 The limitation of FIGAERO temperature ramps to 250 ˚C may result in further error as some SCOs may not be fully desorbed from the filter due to their low vapour pressures. To evaluate the mass left on a filter, several double desorption cycles were performed where mass is collected and desorbed such as in standard use. This is performed by re-heating the same filter once cooled to attain a second thermogram of the same filter. The second thermogram exhibited an average of 90% reduction of counts for the SCO, although the NOSs had an average decrease of 82% counts. This

10 indicates that most, but not all mass, are removed from the filters when desorbing. For the interpretation of the results of the field campaign this effect will induce a small distortion on the time evolution of SCOs when comparing to other parameters, e.g. 9% of NOSs will remain on the filter and being subjected to the subsequent desorption cycle.

2.5.3 Offline and online measurement comparison of SCOs

15 Filter measurements, for orbitrap and HPLC MS analysis, were taken diurnally at the same sampling site, although from a different inlet and location in the building. The CIMS hourly desorption data was averaged over corresponding collection period to attain a day and nighttime CIMS data point. The period between the 23rd May and 1st June was selected due to all instrument measurements being undisturbed during this period. It must be noted that CIMS data is lacking one data point daily while the background filter measurements were taken. The CIMS, orbitrap and HPLC do

20 not measure all of the same species. Here a comparison of total 5 ions is presented with the HPLC and 2 from the orbitrap, where a further extensive comparison is to be performed in an accompanying manuscript. Figure SI3 illustrates the time series of CIMS (hourly and diurnal) measurements of GAS and IEPOX sulfate alongside the HPLC measurements. The diurnal data agrees well with an R value of 0.78 and 0.82 for GAS and IEPOX sulfate respectively. The sum of the time series we have multi instrument data for (GAS; IEPOX sulfate, LAS, $C_4H_7SO_7$, $C_5H_{11}SO_7$ and

25 $C_5H_7SO_7$) for HPLC and $C_9H_{11}SO_5$ and $C_9H_8SO_5$ for orbitrap is displayed in the top panel. In general, the time series agree well and also have a good correlation (R = 0.7 and 0.81 for HPLC and orbitrap respectively) illustrating the ability for CIMS to agree with the offline methods and measure the SCOs accurately at low and high time resolution.

30 **2.7 Knudsen Effusion Mass Spectrometer (KEMS)**

The KEMS technique was utilized to measure the vapour pressure of SCOs observed in the gas phase measurements by the CIMS. The KEMS technique is able to measure vapour pressures from 10^{-1} to 10^{-8} Pascals (Pa) ranging from

volatile organic compounds to extremely low volatility organic compounds. A full description of the technique can be found in Booth *et al*. (2009, 2010) and the measurements of a series of compounds over a large VP range, in a recent inter-comparison study from this instrument, can be found in Krieger *et al*. (2017). Briefly, the instrument consists of a temperature controlled Knudsen effusion cell, suitable for controlled generation of a molecular beam of the sample organic compounds in a vacuum chamber, coupled to a quadrupole mass spectrometer. The cell has a chamfered effusing orifice with a size ≤1/10 the mean free path of the gas molecules in the cell. This ensures the orifice does not significantly disturb the thermodynamic equilibrium of the samples in the cell (Hilpert, 2001). The system is calibrated using the mass spectrometer signal from a sample of known vapour pressure, in this case malonic acid (vapour pressure at 298K = 5.25×10^{-4} Pa, (Booth *et al*., 2012)). A load-lock allows the ioniser filament to be left on, then a new sample of unknown vapour pressure can be measured. Solid state vapour pressures measured in the KEMS can then be converted to sub-cooled liquid vapour pressures using the melting point, enthalpy and entropy of fusion, which are obtained by using a Differential Scanning Calorimeter (DSC) (TA instruments Q200).

3. Concentrations and partitioning of atmospheric SCOs

3.1 SCO contribution to PM$_1$ at Changping

The SCOs measured at the Changping site had a mean campaign concentration of 210 ± 110 ng m^{-3} (Table 1). The highest concentration of total SCOs during the campaign was 540 ng m^{-3} and the lowest 40 ng m^{-3}, thus they are omnipresent and have significant sources during most atmospheric conditions. These concentrations are consistent with Stone *et al*. (2012) reporting an average SCO concentration of 700 ng m^{-3} in a number of rural and urban sites in Asia. A mean SCO contribution to OA in the work presented here was calculated to be $2.0 \pm 1\%$ (Table 1), within the range of values calculated by Stone *et al*. (2012) (0.8% to 4.5%), further supporting evidence that SCO contribution to PM$_1$ mass is relatively low in Asia. The CIMS cannot claim to measure total SCO, rather than singularly identify and measure SCOs contributing to the total mass loading. Therefore, the SCO contribution reported in this work should be considered as a lower limit. The Liao *et al*. (2015) study also supports the idea that SCO contribution to PM$_1$ mass in anthropogenically dominated regions is less significant than that from biogenically dominating air masses by observing a significantly higher contribution of IEPOX sulfate to PM$_1$ mass on the East coast of the United States (1.4%) than the West Coast (0.2%).

The observation of higher relative contribution of SCOs to total organics in more remote regions compared to a densely populated urban area, supports the idea that SCOs provide a higher contribution to PM in aged air due to their secondary production pathways. Similar to Lahore (as studied by Stone *et al*., 2012), Beijing has many strong primary anthropogenic sources which will dominate the mass loading and therefore, initially, will contribute to a lower fraction

of the total concentration from secondary production due to limited processing near the source. Throughout the campaign, a good correlation (R^2 = 0.66) was observed between an increase in ΔSCO mass and PM_1 mass, although the SCO contribution to PM_1 decreased exponentially (Figure 3) indicating that the pollution episodes contain a lower fraction of SCOs with respect to total PM_1. This result suggests that SCO do not play as large a role as expected even though their precursors (organics and sulfate) are abundant within the episodes, indicating the conditions of their formation may be more vital than absolute concentrations of precursors.

3.2 Gas to particle phase partitioning of SCOs

The FIGAERO ToF-CIMS data exhibited indication of SCOs in both the particle and gas phase. Previous studies have supported the existence of e.g. gas phase GAS in ambient air (e.g. Ehn *et al*., 2010), although some work has attributed other measurement techniques detection of gas phase SCO to result from measurement artefacts (Hettiyadura *et al*., 2017; Kristensen *et al*., 2016). Once all HR peaks have been identified, the batch fitting and HR time series for the whole data set is processed and then separated into gas phase measurements and particle phase desorption profile time series. The data is background corrected i.e., subtraction of both the gas phase background periods and blank filter desorption's. Upon analysis of the resultant data, significant concentrations of gas phase SCOs were observed. Figure 4 depicts the overall sum SCO mass concentration time series in the gas and particle phase. The mean contribution from gas phase SCO to total SCO was found to be 11.6%, 23±8 ng m^{-3}. This suggests a significant amount of SCO is always present in the gas phase and factors that influence gas-to-particle partitioning influence the level of this contribution. These changes in contribution also reduce the possibilities for memory effect , e.g. one possibility is the deposition of SCOs onto the IMR walls during the temperature ramp of the desorption which in time may de-gas and be observed in the gas phase. This would likely result in a constant ratio of particle to gas phase concentrations and would likely cause a hysteresis in the observed gas phase measurements with respect to the particle phase, which was not observed.

The vapour pressure of NP OS was measured using the KEMS instrument in the laboratory to establish the existence of gas phase SCOs. This technique has recently been employed to measure the vapour pressure of NP (Bannan *et al*., 2017). The KEMS experiments found the solid state vapour pressure of NP OS to be 5.07×10^{-5} Pa at 298 K. Assuming an average subcooled liquid correction for all compounds measured in the Bannan *et al*. (2017) study, as no DSC data is available, the subcooled liquid vapour pressure of NP OS is 2.32×10^{-4} (Pa). This vapour pressure lies within the semi volatile organic compound range, therefore supporting the potential partitioning of SCOs to the gas phase under ambient conditions. To further validate the CIMS and KEMS findings, one can evaluate different compounds VPs from the FIGAERO data utilizing the T_{max} and compare to literature values. The CIMS, using T_{max}, estimated VPs of malonic, succinic and glutaric acid to be 2×10^{-3}, 1.85×10^{-3}, 1×10^{-3} Pa which compare well to values presented by Bilde *et al*. (2015) VPs; 6.2×10^{-3}, 1.3×10^{-3}, 1×10^{-3}. Using this agreement for well-known substances we notice the T_{max} of SCO to be in the range were it can provide significant gas-phase concentration. Still, the observed presence of gas phase GAS

and IEPOX-OS does not agree with previous studies of these compounds (Stone *et al.,* 2012, Hettiyadura *et al.*, 2017). Therefore, one need to be cautious and deeper analysis into exact VPs and partitioning from the present work must be performed to assess whether their gas phase presence could be fully confirmed. So far we note that fragmentation of organic species (oligomers) during desorption could lead to a potential artefact and a lower T_{max} at a monomer peak (Stark *et al*., 2017 and Lopez-Hilfiker *et al.*, 2016). However, here we identify and expect no dimers or oligomers that could fragment to form the SCOs identified. Furthermore, the higher mass organics are likely to have a much higher VP than the lower mass SCO and provide a second T_{max} which would produce a lower VP value due to the greater energy required to break the bonds. Analysis of T_{max} throughout the campaign shows no double peak thermograms and an acceptable stability of T_{max}(SI4). T_{max} varied by up to 14 Celsius and appeared to correlate well with particulate loading, similar to that observed by Huang *et* al*.,* (2017), who suggested that this is a result of diffusion limitations within the particle matrix. If the data is tentatively analyzed to assess mechanism regarding their partitioning, aerosol liquid water content would affect the partitioning of gas phase compounds to aerosols (Zhang *et al*., 2007). Data point size coding the correlation of the gas and particle phase SCO concentrations indicates partitioning towards the aerosol phase at lower relative humidities (Figure 4). Conversely, as temperature increases (as indicated by red colour shading) the SCOs partition further towards the gas phase, as thermodynamically expected.

Further work is necessary to validate these findings and determine the mechanisms and importance of gas phase SCO abundance in ambient air. For example, the high contribution in the gas phase could be perturbed if equilibrium between condensation to particle phase and gas phase formation has not been established. It must be noted that the a correct calibration of T_{max} with VP would be necessary to extract such information, but qualitatively the relative VP compared to NP OS could be utilized as a reliable scale due its independent calibration by KEMS.

4. Sources and secondary formation of SCOs

4.1 SCO sources at the Changping site

SCOs are known to have biogenic and anthropogenic sources and some which have multiple sources from both, e.g. GAS (Hettiyadura *et al.,* 2017; Hansen *et al*., 2014). Burning events are known to emit high levels of organics and nitrates and potentially sulfur, depending on the type of fuel used. This enables biomass burning to be a potential anthropogenic and biogenic source of SCOs. The site at Changping was influenced by both regional anthropogenic pollution from the Beijing area and localized anthropogenic activity (industry, biomass burning and traffic) but also emissions from biogenic sources, as it is situated in a semi-rural area, with forest, vegetation and plantations. This was evident from the benzene and isoprene PTR-MS measurements which have mean campaign concentrations of 0.55 $\pm$ 0.4 and 0.27 $\pm$ 0.19 ppb respectively with maxima of 5 and 1.5 ppb respectively. Thus, as shown in Figure 5, PTR-MS

measurements mean daily concentrations were utilized to evaluate if the ratio benzene and isoprene can indicate a higher mass loading and contribution of aromatic and biogenic SCOs measured in this work. Data on days with incomplete time series have been removed to ensure the data presented represents a full mean of the day concentration. A good correlation between the benzene:isoprene ratio and sum of SCOs is observed. It suggests an increase in relative anthropogenic emissions promotes an increase in total SCO loading. It should be noted that $C_6H_{10}SO_7$ has no known precursor in the literature, although it contributes significantly to the SCO mass loading in this work (16%).

4.1.1 Biogenic and anthropogenic SCOs

Biogenic SCOs are known to be comprised of monoterpene, sesquiterpene and isoprene derived SCOs which have been identified in rural, sub-urban and urban areas around the world, and have been shown to be a major constituent of SOA (Surratt et al., 2008; Shalamzari et al., 2014, Liao et $al.,$ 2015). IEPOX sulfate is commonly found to be the most dominant SCO at many locations and was identified also at the Changping site. The IEPOX sulfate mean concentration represented 0.11% of the OA mass, agreeing well with concentrations found in Western USA (significant anthropogenic emissions) and lower than the Eastern USA as expected due to higher biogenic and isoprene emissions (Liao et $al.,$ 2015). Although IEPOX sulfate is considered one of the most abundant individual organic molecules in aerosols (Chan et al., 2010), here our results show it only contributed to 2% of the SCO mass and was the 8th most abundant SCO in the particle phase. Additionally, two other isoprene derived SCOs, $C_5H_8SO_7$ and $C_4H_8SO_7$, were measured by the CIMS with mean campaign concentrations of 2 and 3 ng m^{-3} respectively and a contribution of 0.02% to OA mass. The highest contributing biogenic SCO to the ambient air was a NOS, $C_{10}H_{16}NSO_7$, a known NOS derived from alpha-pinene oxidation. This NOS had a mean campaign concentration of 21 ng m^{-3} and a 0.2% contribution to OA mass.

Anthropogenic SCOs, including polyaromatic hydrocarbon (PAH) derived SCOs have received more attention in recent studies due to their identification (Nozière et al., 2010; Hansen et al., 2015). Aromatic SCOs and sulfonates have only recently been identified as atmospherically abundant SCOs (Riva et $al.,$ 2015). In this work we find that the PAH derived SCO $C_{11}H_{11}SO_7$ is the most dominant SCO in Beijing with a mean concentration of 40 ng m^{-3}, contributing to 20% of the total SCO mass and 0.4% of the OA mass. This SCO has been identified in laboratory studies as an SCO forming from the photo-oxidation of 2-methyl napthalene, one of the most abundant gas phase PAHs and is thought to represent a missing source of urban SOA (Riva et $al.,$ 2015). This work presents the possible significance of PAH SCOs in Beijing and further evidence that photo-oxidation of PAHs represents a greater SOA potential than currently recognized. A further 8 anthropogenic aromatic derived SCOs were identified as common components of the PM$_1$ representing more than half of the total SCOs with $C_7H_5SO_4$ contributing to 24 ng m^{-3} and 0.23% OA mass. The total anthropogenic related SCOs had a mean mass of 120 ng m^{-3} and contributed to 1.2% of the OA mass.

4.1.2 Biomass burning source of SCOs

NP (a product of benzene oxidation and nitration) has previously been detected in the gas and aerosol phase (Harrison *et al.,* 2005) and is an important component of brown carbon (Mohr *et al.,* 2013). NP has primary sources, such as vehicle exhausts and biomass burning (Inomata *et al.,* 2013 and Mohr *et al.,* 2013) and secondary sources via the photo-oxidation of aromatic hydrocarbons in the atmosphere (Harrison *et al.,* 2005). High levels on anthropogenic activity, biomass burning and strong photochemistry in Beijing therefore enable this region to be a strong potential source of NP. Both NP and NP OS diurnal profiles exhibit an increase in the morning (6am onwards) although NP OS appears to increase in concentration more rapidly. The early morning biomass burning and anthropogenic activity are likely to contribute to production of both species, although the higher sulphate content of the biomass burning emissions may promote a faster production of NP OS and conversion of NP to NP OS. Both compounds continue to increase with a photochemical profile with one peak at midday but also a peak around 4pm, likely to be a second source of the day from anthropogenic activity. The NP OS continues to increase until sunset, which could result from further photochemical production from the NP emitted throughout the day whereas NP falls off after the 4pm peak. The campaign time series for NP and NP OS can be seen in Figure 6. Unlike its precursor and most other pollutant markers measured in this work, including all other SCOs, NP OS exhibits higher concentrations between 17th to the 22nd May compared to the 28th May to 3rd June. The only compound with a similar campaign profile is acetonitrile (a marker for biomass burning), which has significantly enhanced concentrations between 6 and 8am from the 17th to the 22nd May. Back trajectories of these two time periods show the air mass during the first period comes from the west, a more rural region of China and known to be influenced heavily by biomass burning, whereas the second time period has wind directions mainly bringing in air masses that have gone through the Tianjin and Beijing area. It is therefore hypothesized that the NP OS, which peaks later in the day than the NP and acetonitrile, is a secondary product formed from the biomass burning and has aged after being emitted from air masses further away. Here NP can have more local sources of biomass burning and traffic which then can contribute to NP OS production, but at a slower time scale, which in this data set, appears as lower production due to the limited oxidation of local air masses.

4.2 SCO production mechanisms

4.2.1 *Precursor analysis*

The availability of the organic precursors of SCOs is a limiting factor for the SCO production rate. The measurement of the precursors in the gas and particle phase by CIMS enables a more descriptive mechanism to be outlined as the partitioning of the precursor will vary the distribution between gas and particle production pathways and therefore rate of corresponding SCO production. Glycolic acid has on average 75% of its mass in the gas phase for the measurement period whereas GAS is dominantly in the particle phase (Figure 7). The GAS particle phase concentration is observed to increase as the SO_4^{2-} mass loading increases and the GA gas and particle concentrations increase, although the

partitioning of the GA towards the gas phase restricts the SCO production. This can be seen in Figure 7 as for a given SO_4^{2-} concentrations, the data with warm colors (red), representing high fraction of precursor GA in particle phase, generally provides higher concentration of particulate GAS.

The main formation mechanism of GAS is thought to be via the reaction of GA in the gas phase with an acidic aerosol sulfate (Liao *et al*., 2016), contrary to what is observed here. Although an increase in GAS is observed to correlate with the GA, it appears that a partitioning towards the particle phase promotes GAS production. An R^2 correlation of 0.68 between GAp and GASp whereas an R^2 of 0.4 is observed between GAg and GASp.

The sum of benzene SCOs exhibits a good correlation to the gas phase benzene time series (Figure 8), although their abundance should also rely on the availability of sulfur in the particle phase and the age of the air mass, if it is assumed that they are formed via secondary reactions of primary pollutants. In order to assess how the SCO production rates may vary due to these factors, two distinct high benzene SCO events with similar benzene concentrations were scrutinized, i.e. the 29th May and the 1st June. The first period has lower SO_4^{2-} concentrations, higher H_2SO_4 levels and a higher total benzene SCO concentration. The exact age (or time for oxidation) of compounds in an air mass are without an extensive modelling study complicated to derive. However, as proxies to attain an approximation about oxidation state one may use some trace compounds. Monoterpene oxidation by the hydroxyl radical (OH) or O_3 results in the formation of multifunctional organic acids such as pinonic acid which can then be further oxidised by OH to form 3-methyl-1,2,3-butane-tricarboxylic acid (MBTCA), both of which are measured by CIMS. Therefore, in an air mass containing monoterpene emissions, as known here through the identification of their products such as $C_{10}H_{16}NO_7S$, we can utilize the ratio of pinonic acid and MBTCA; as tracers of monoterpene SOA processing as detected in ambient aerosols in Europe, USA and Amazon (Gao *et al*., 2006) as a relative photochemical clock. During the high benzene event on the 1st June, according to the pinonic acid: MBTCA ratio, the air mass is less oxidized relative to the air mass on the 29th May (Figure 8). This would allow less time for secondary production and explain the relatively lower concentration of SCOs, irrespective of higher SO_4^{2-} concentrations and similar benzene concentrations.

To further elaborate The Gothenburg Potential Aerosol Mass (Go:PAM) reactor (Watne et al, 2018) was tested and utilized to simulate aging of the air mass during periods of the campaign. Here the ratio between pinonic acid and MBTCA was observed to increase by an average of 3 during aging within the Go:PAM which has been calculated to be the OH exposure equivalent of 2 days in the ambient atmosphere. As this ratio increased with aging, the SCO concentration also increased exponentially, further supporting the secondary production of SCO in photochemically aged air mass. Although limited data is available here for simultaneous Go:PAM and CIMS measurements, the results indicate the potential utilization of the chamber to probe secondary production processes.

4.2.2 *Aerosol acidity*

The molecular ion $H_3S_2O_7^-$ was identified in the mass spectra throughout the campaign, which has previously been detected by Liao *et al.* (2015) using a Particle Analysis Laser Mass Spectrometer to measure SCOs. They attribute this mass to be a cluster of HSO_4^- with sulfuric acid (H_2SO_4). Particles in the presence of H_2SO_4, and therefore high acidity, form this cluster whereas neutralized ions are likely to favour the unclustered HSO_4^- form. Therefore, the ratio between the cluster and the bisulfate ion increases with increasing aerosol acidity (Murphy *et al.*, 2007; Carn *et al.*, 2011). Liao *et al.* (2015) validate the appropriateness of this cluster as a marker for aerosol acidity thorough comparisons to a thermodynamic model with gas and aerosol phase measurement inputs. Acidity was also calculated utilizing the gas and particle phase H_2SO_4 and liquid H^+ ion concentration analysed using an offline technique, as described by Guo *et al.* (2010), from diurnal samples taken at the site. This method showed good agreement with the integrated diurnal counts of the $H_3S_2O_7^-$ ion. Therefore, we employ the $HSO_4^-.H_2SO_4^-$ cluster in this work as a qualitative scale for particle acidity utilizing similar assumptions. Figure 9 shows how total SCO mass concentration generally increased as total organic mass from the AMS increased. The correlation indicates that higher acidity (darker colours) tends to promote formation of SCOs when in the presence of high levels of organics and SO_4^{2-} (larger symbol sizes), supporting the growing consensus that aerosol acidity plays an important role in ambient SCO formation. This importance of acidity agrees well with both the acid-catalyzed epoxydiol ring opening formation mechanism (Surratt *et al.*, 2010) and the sulfate radical initiated SCO formation because efficient formation of sulfate radicals also requires acidity (Schindelka *et al.*, 2013).

5. Conclusions

The FIGAERO ToF-CIMS was successfully utilized for the ambient detection of 17 SCOs in Beijing in the gas and aerosol phase with limits of detection in the ng m^3 range. Good agreement with offline filter measurements further supports the robustness of this method for high and low time resolution measurements of SCOs. Further calibrations and comparisons to total SCO measurements are required to evaluate its performance limitation with regards to sensitivity application and peak identification. The SCOs measured by CIMS contributed to 2% of the OA at the semi-rural site, highlighting the relatively low contribution of SCOs in Beijing, an anthropogenically dominated environment. This calculation from CIMS may only be valid to infer each individual SCO contribution to total SOC mass as limitations in SCO identification and quantification limit the CIMS ability for total SCO measurements. Significance of their secondary production pathway prevailed, although still present in relatively fresh air masses. Contributions of SCO to total organics ($2.0 \pm 1\%$), sulfate ($15 \pm 19\%$) and PM ($1.0 \pm 1.4\%$) indicate the concentrations observed in Beijing result from highly processed ambient air masses.

Gas phase SCOs were identified for all the SCOs measured at the site, contributing to in average to 12% of the total SCO mass. The possibility of gas phase SCOs in ambient air was supported by KEMS vapour pressure measurements of NP OS and derived T_{max} values which suggest a vapour pressure in the semi volatile range. The partitioning towards the gas phase was more efficient at high atmospheric temperatures, while lower relative humidities promoted partitioning to the particle phase.

Biogenic SCOs contributed to a small fraction of the total SCO mass at Changping and was dominated by an α-pinene derived OS with 0.2% contribution to the OA mass. IEPOX sulfate was only the 8th most abundant SCO measured, contrary to common reports that it is one of the most abundant SCO. Anthropogenic precursors contributed to more than half of the SCO mass loading with a PAH derived SCO contributing to as much as 1.2% of the OA mass. Benzene derived SCOs correlated well with gas phase benzene levels and were heavily influenced by photochemical aging. The contribution of each benzene derived SCO to total benzene derived SCO mass varied daily and throughout the campaign highlighting the complexity of the atmospheric processing and composition of SCO. Significant contributions from aromatic SCOs highlight the importance of anthropogenically emitted organics in the Beijing region and their contribution to the Beijing outflow and subsequent photochemistry. NP OS was attributed to biomass burning emissions due to co-occurrence with high levels of acetonitrile. This highlights the importance of anthropogenic emissions and their contribution to SOA from the urban Beijing outflow.

A qualitative CIMS marker for aerosol acidity highlighted the increase in SCO production rate in acidic aerosols in the presence of high SO_4^{2-} and organics. The correlation of SCO production and RH becomes more complex for individual SCOs, which cannot be resolved within this studies framework.

Acknowledgement:

The work was done under the framework research program on 'Photochemical smog in China" financed by Swedish Research Council (639-2013-6917). The National Natural Science Foundation of China (21677002) and the National Key Research and Development Program of China (2016YFC0202003) also helped fund this work.

References

Bannan, T. J., Booth, A. M., Jones, B. T., O'Meara, S., Barley, M. H., Riipinen, I., Percival, C. J., and Topping, D.: Measured saturation vapor pressures of phenolic and nitro-aromatic compounds, Environ. Sci. Technol., 51 (7), 3922–3928, 2017.

Booth, A. M., Markus, T., McFiggans, G., Percival, C. J., Mcgillen, M. R., and Topping, D. O.: Design and construction of a simple Knudsen Effusion Mass Spectrometer (KEMS) system for vapour pressure measurements of low volatility organics, Atmos. Meas. Tech., 2, 355–361, 2009.

Booth, A. M., Barley, M. H., Topping, D. O., McFiggans, G., Garforth, A., and Percival, C. J.: Solid state and sub-cooled liquid vapour pressures of substituted dicarboxylic acids using Knudsen Effusion Mass Spectrometry (KEMS) and Differential Scanning Calorimetry, Atmos. Chem. Phys., 10, 4879–4892, 2010.

Booth, A. M., Bannan, T., Barley, M. H., Topping, D. O., McFiggans, G., and Percival, C. J.: The role of ortho, meta, para isomerism in measured solid state and derived sub-cooled liquid vapour pressures of substituted benzoic acids, Roy. Soc. Chem., 2, 4430-4443, 2012.

Boris, A. J., Lee, T., Park, T., Choi, J., Seo, S. J., and Collet Jr, J. L.: Fog composition at Baengnyeong Island in the eastern Yellow Sea: detecting markers of aqueous atmospheric oxidations, Atmos. Chem. Phys., 16, 437-453, 2016.

Bruggemann, M., Poulain, L., Held, A., Stelzer, T., Zuth, C., Richters, S., Mutzel, A., van Pinxteren, D., Iinuma, Y., Katkevica, S., Rabe, R., Herrmann., and Hoffmann, T.: Real-time detection of highly oxidized organosulfates and BSOA marker compounds during the F-BEACh 2014 field study, Atmos. Chem. Phys., 17, 1453–1469, 2017.

Carn, S. A, Froyd, K. D., Anderson, B. E., Wennberg,P., Crounse, J., Spencer, K., Dibb, J. E., Krotkov, N. A., Browell, E. V., Hair, J. W., Diskin, G., Sachse, G., and Vay, S.: A. In situ measurements of tropospheric volcanic plumes in Ecuador and Colombia during TC4, J. Geophys. Res., 116, D00J24, 2011.

Chan, M. N., Surratt, J. D., Claevs, M., Edgerton, E. S., Tanner, R. L., Shaw, S. L., Zheng, M., Knipping, E. M., Eddingsaas, N. C., Wennberg, P. O., and Seinfeld, J. H.: Characterization and quantification of isoprene-derived epoxydiols in ambient aerosol in the Southeastern United States, Environ. Sci. Technol., 44,12, 4590–4596, 2010.

de Gouw, J. and Warneke, C.: Measurements of volatile organic compounds in the earths atmosphere using proton-transferreaction mass spectrometry, Mass Spectrom. Rev., 26, 223–257, 2007.

DeCarlo, P. F., Kimmel, J. R., Trimborn, A., Northway, M. J., Jayne, J. T., Aiken, A. C., Gonin, M., Fuhrer, K., Horvath, T., and Docherty, K. S.: Field-deployable, high-resolution, time-of-flight aerosol mass spectrometer, Anal. Chem., 78, 8281–8289, 2006.

Ehn, M., Junninen, H., Petaj a, T., Kurtén, T., Kerminen, V.-M., Schobesberger, S., Manninen, H. E., Ortega, I. K., Vehkamäki, H., Kulmala, M., and Worsnop, D. R.: Composition and temporal behavior of ambient ions in the boreal forest, Atmos. Chem. Phys., 10, 8513–8530, 2010.

Ehn, M., Thornton, J. A., Kleist, E., Sipila, M., Junninen, H., Pullinen, I., Springer, M., Rubach, F., Tillmann, R., Lee, B., LopezHilfiker, F., Andres, S., Acir, I.-H., Rissanen, M., Jokinen, T., Schobesberger, S., Kangasluoma, J., Kontkanen, J., Nieminen, T., Kurtén, T., Nielsen, L. B., Jørgensen, S., Kjaergaard, H. G., Canagaratna, M., Maso, M. D., Berndt, T., Petaja, T., Wahner, A., Kerminen, V.-M., Kulmala, M., Worsnop, D. R., Wildt, J., and Mentel, T. F.: A large source of low-volatility secondary organic aerosol, Nature, 506, 476–479, 2014.

Foley, K. M., Roselle, S. J., Appel, K. W., Bhave, P. V., Pleim, J. E., Otte, T. L., Mathur, R., Sarwar, G., Young, J. O., Gilliam, R. C., Nolte, C. G., Kelly, J. T., Gilliland, A. B., and Bash, J. O.: Interactive comment on "Incremental testing of the community multiscale air quality (CMAQ) modeling system version 4.7", Geosci. Model Dev. Discuss., 2, C515–C532, 2010.

Gao, S., Surratt, J. D., Knipping, E. M., Edgerton, E. S., Shahgholi, M., and Seinfeld, J. H.: Characterization of polar organic components in fine aerosols in the southeastern United States: Identity, origin, and evolution, J. Geophys. Res. Atmos., 111, D07302, 2006.

Gómez-González, Y., Surratt, J. D., Cuyckens, F., Szmigielski, R., Vermeylen, R., Jaoui, M., Lewandowski, M., Offenberg, J. H., Kleindienst, T. E., Edney, E. O., Blockhuys, F., Van Alsenoy, C., Maenhaut, W., and Claeys, M.: Characterization of organosulfates from the photooxidation of isoprene and unsaturated fatty acids in ambient aerosol using liquid chromatography/(-) electrospray ionization mass spectrometry, J. Mass Spectrom., 43, 371–382, 2008.

Guo, S., Hu, M., Wang, Z. B., Slanina, J., and Zhao, Y. L.: Size-resolved aerosol water-soluble ionic compositions in the summer of Beijing: implication of regional secondary formation, Atmos. Chem. Phys.,10, 947-959, 2010.

Guo, S., Hu, M, Guo, Q. F., Zhang, X., Zheng, M., Zheng, J., Chang, C. C., Schauer, J. J., and Zhang, R. Y.: Primary sources and secondary formation of organic aerosols in Beijing, China, Environ. Sci. Technol., 46, 18, 9846-9853, 2012.

Guo, S., Hu, M., Guo, Q. F., Zhang, X., Schauer, J. J., and Zhang R. Y.: Quantitative evaluation of emission control of primary and secondary organic aerosol sources during Beijing 2008 Olympics, Atmos. Chem. Phys., 13, 8303–8314, 2013.

Guo, S., Hu, M., Zamora, M, Peng, J. F., Shang, D. J., Zheng, J., Du Z. F., Wu, Z. J., Shao, M., Zeng, L. M., Molina, M., and Zhang, R.: Elucidating severe urban haze formation in China, PNAS, 111, 49, 17373-17378, 2014.

Hallquist, M., Wenger, J. C., Baltensperger, U., Rudich, Y., Simpson, D., Claeys, M., Dommen, J., Donahue, N. M., George, C., Goldstein, A. H., Hamilton, J. F., Herrmann, H., Hoffmann, T., Iinuma, Y., Jang, M., Jenkin, M. E., Jimenez, J. L., Kiendler-Scharr, A., Maenhaut, W., McFiggans, G., Mentel, Th. F., Monod, A., Prévôt, A. S. H., Seinfeld, J. H., Surratt, J. D., Szmigielski, R., and Wildt, J.: The formation, properties and impact of secondary organic aerosol: current and emerging issues, Atmos. Chem. Phys., 9, 5155–5236, doi:10.5194/acp-9-5155- 2009, 2009.

Hallquist, M., Munthe, J., Hu, M., Mellqvist, J., Wang, T., Chan, C. K., Gao, J., Boman, J., Guo, S., Hallquist, Å. M., Moldanova, J., Pathak, R. K., Pettersson, J. B. C., Pleijel, H., Simpson, D., and Thynell, M.: Photochemical smog in china: Scientific challenges and implications for air quality policies, Nat. Sci. Rev., 3, 401-403, 2016.

Hansen, A. M. K., Kristensen, K., Nguyen, Q. T., Zare, A., Cozzi, F., Nøjgaard, J. K., Skov, H., Brandt, J., Christensen, J. H., Ström, J., Tunved, P., Krejci, R., and Glasius, M.: Organosulfates and organic acids in Arctic aerosols: speciation, annual variation and concentration levels, Atmos. Chem. Phys., 14, 7807–7823, 2014.

Hansen, A. M. K., Hong, J., Raatikainen, T., Kristensen, K., Ylisirniö, A., Virtanen, A., Petäjä, T., Glasius, M., and Prisle, N. L.: Hygroscopic properties and cloud condensation nuclei activation of limonene-derived organosulfates and their mixtures with ammonium, Atmos. Chem. and Phys., 15, 14071-14089, 2015.

Harrison, M. A. J., Barra, S., Borghesi, D., Vione, D., Arsene, C., and Iulian Olariu, R.: Nitrated phenols in the atmosphere: a review, Atmos. Environ., 39, 231–248, 2005.

Heald, C. L., Jacob, D. J., Park, R. J., Russell, L. M., Huebert, B. J., Seinfeld, J. H., Liao, H., and Weber, R. J.: A large organic aerosol source in the free troposphere missing from current models, Geophys. Res. Lett., 32, L18809, 2005.

Hettiyadura, A. P. S., Stone, E. A., Kundu, S., Baker, Z., Geddes, E., Richards, K., and Humphry, T.: Determination of atmospheric organosulfates using HILIC chromatography with MS detection, Atmos. Meas. Tech., 8, 2347–2358, 2015.

Hettiyadura, A. P. S., Jayarathne, T., Baumann, K., Goldstein, A. H., de Gouw, J. A., Koss, A., Keutsch, F. N., Skog, K., and Stone, E. A.: Qualitative and quantitative analysis of atmospheric organosulfates in Centreville, Alabama, Atmos. Chem. Phys., 17, 1343-1359, 2017.

Hilpert, K.: Potential of mass spectrometry for the analysis of inorganic high temperature vapors, Fresen. J. Anal. Chem., 370, 471–478, 2001.

Hu, W., Hu, M., Jiminez, J. L., Tang, Q., Peng, J. F., Hu, W., Shao, M., Wang, M., Zeng, L. M., Wu, Y. S., Gong, Z. H., Huang, X. F., and He, K. Y.: Insights on organic aerosol aging and the influence of coal combustion at a regional receptor site of central eastern China, Atmos. Chem. Phys., 13, 10095-10112, 2013.

Hu, W., Hu, M., Hu, W., Jimenez, J. L., Yuan, B., Chen, W., Wang, M., Wu, Y., Chen, C., Wang, Z., Peng, J., Yang, K., Zeng, L., and Shao, M.: Chemical composition, sources and aging process of sub-micron aerosols in Beijing: contrast between summer and winter, J. Geophys. Res. Atmos., 121, 1955–1977, 2016.

Hu, W., Hu, M., Hu, W. W., Zheng, J., Chen, C., Wu, Y., and Guo, S.: Seasonal variations of high time-resolved chemical compositions, sources and evolution for atmospheric submicron aersols in the megacity Beijing, Atmos. Chem. Phys. Discuss., 2017, 1-43, 2017.

Huang, D. D., Li, Y. J., Lee, B. P., and Chan, C. K.: Analysis of Organic Sulfur Compounds in Atmospheric Aerosols at the HKUST Supersite in Hong Kong Using HR-ToF-AMS, Environ. Sci. Technol., 49, 3672–3679, 2015.

Huang, X. F., He, L. Y., Hu, M., Canagaratna, M. R., Sun, Y., Zhang, Q., Zhu, T., Xue, L., Zeng, L. W., Liu, X. G., Zhang, Y. H., Jayne, J. T., Ng, N. L., and Worsnop, D. R.: Highly time-resolved chemical characterization of atmospheric submicron particles during 2008 Beijing olympic games using an Aerodyne high-Resolution aerosol mass spectrometer, Atmos. Chem. Phys., 10(18), 8933-8945, 2010.

Iinuma, Y., Muller, C., Berndt, T., Boge, O., Claeys, M., and Herrmann, H.: Evidence for the existence of organosulfates from beta-pinene ozonolysis in ambient secondary organic aerosol, Environ. Sci. Technol., 41, 19, 6678-6683, 2007.

Inomata, S., Tanimoto, H., Fujitani, Y., Sekimoto, K., Sato, K., Fushimi, A., Yamada, H., Hori, S., Kumazawa, Y., Shimono, A., and Hikida, T.: On-line measurements of gaseous nitro-organic compounds in diesel vehicle exhaust by proton-transfer-reaction mass spectrometry, Atmos. Environ., 73, 195–203, 2013.

Jokinen, T., Sipilä, M., Richters, S., Kerminen, V.-M., Paasonen, P., Stratmann, F., Worsnop, D., Kulmala, M., Ehn, M., Herrmann, H., and Berndt, T.: Rapid autoxidation forms highly oxidized RO2 radicals in the atmosphere, Angew. Chem. Int. Edit., 53, 14596–14600, doi:10.1002/anie.201408566, 2014.

Kim, J. Y., Lee, E. Y., Choi, I., Kim, J., and Cho, K. H.: Effects of the particulate matter2.5 (PM1) on lipoprotein metabolism, uptake and degradation, and embryo toxicity, Mol Cells., 38, 12, 1096-1104, 2015.

Krieger, U. K., Siegrist, F., Marcolli, C., Emanuelsson, E. U., Gøbel, F. M., Bilde, M., Marsh, A., Reid, J. P., Huisman, A. J., Riipinen, I., Hyttinen, N., Myllys, N., Kurtén, T., Bannan, T., and Topping, D.: A reference data set for validating vapor pressure measurement techniques: Homologous series of polyethylene glycols, Atmos. Meas. Tech. Discuss., https://doi.org/10.5194/amt-2017-224, in review, 2017.

Kristensen, K. and Glasius, M.: Organosulfates and oxidation products from biogenic hydrocarbons in fine aerosols from a forest in North West Europe during spring, Atmos. Environ., 45, 4546–4556, 2011.

Kristensen, K., Bilde, M., Aalto, P. P., Petäjä, T., and Glasius, M.: Denuder/filter sampling of organic acids and organosulfates at urban and boreal forest sites: gas/particle distribution and possible sampling artifacts. Atmos. Environ., 130, 36-53, 2016.

Lee, B. H., Mohr, C., Lopez-Hilfiker, F. D., Lutz, A., Hallquist, M., Lee, L., Romer, P., Cohen, R. C., Iyer, S., Kurtén, T., Hu, W., Day, D. A., Campuzano-Jost, P., Jimenez, J. L., Xu, L., Ng, N. L., Guo, H., Weber, R. J., Wild, R. J., Brown, S. S., Koss, A., de Gouw, J., Olson, K., Goldstein, A. H., Seco, R., Kim, S., McAvey, K., Shepson, P. B., Starn, T., Baumann, K., Edgerton, E. S., Liu, J., Shilling, J. E., Miller, D. O., Brune, W., Schobesberger, S., D'Ambro, E. L., and Thornton, J. A.: Highly functionalized organic nitrates in the southeast United States: Contribution to secondary organic aerosol and reactive nitrogen budgets, P. Natl. Acad. Sci. USA, 113, 1516–1521 doi:10.1073/pnas.1508108113, 2016.

Le Breton, M., McGillen, M. R., Muller, J. B. A., Bacak, A., Shallcross, D. E., Xiao, P., Huey, L. G., Tanner, D., Coe, H., and Percival, C. J.: Airborne observations of formic acid using a chemical ionization mass spectrometer, Atmos. Meas. Tech., 5, 3029–3039, 2012.

Le Breton, M., Bacak, A., Muller, J. B. A., O'Shea, S. J., Xiao, P., Ashfold, M. N. R., Cooke, M. C., Batt, R., Shallcross, D. E., Oram, D. E., Forster, G., Bauguitte, S. J.-B., Palmer, P. I., Parrington, M., Lewis, A. C., Lee, J. D., and Percival, C. J.: Airborne hydrogen cyanide measurements using a chemical ionisation mass spectrometer for the plume identification of biomass burning forest fires, Atmos. Chem. Phys., 13, 9217– 9232, 2013.

Le Breton, M., Bacak, A., Muller, J. B. A., Bannan, T. J., Kennedy, O., Ouyang, B., Xiao, P., Bauguitte, S. J. B., Shallcross, D. E., Jones, R. L., Daniels, M. J. S., Ball, S. M., and Percival, C. J.: The first airborne comparison of N2O5 measurements over the UK using a CIMS and BBCEAS during the RONOCO campaign, Anal. Methods-UK, 6, 9731-9743, 2014.

Li, Y. J., Sun, Y., Zhang, Q., Li, X., Li, M., Zhou, Z., and Chan, C.: Real-time chemical characterization of atmospheric particulate matter in China: A review, Atmos. Environ., 158, 270-304, 2017.

Liao, J., Froyd, K. D., Murphy, D. M., Keutsch, F. N., Yu, G., Wennberg, P. O., St. Clair, J. M., Crounse, J. D., Wisthaler, A., Mikoviny, T., Jimenez, J. L., Campuzano-Jost, P., Day, D. A., Hu, W., Ryerson, T. B., Pollack, I. B., Peischl, J., Anderson, B. E., Ziemba, L. D., Blake, D. R., Meinardi, S., and Diskin, G.: Airborne measurements of organosulfates over the continental U.S, J. Geophys. Res. Atmos., 120, 2990–3005, 2015.

5   Lin, P., Yu, J. Z., Engling, G., and Kalberer, M.: Organosulfates in humic-like substance fraction isolated from aerosols at seven locations in East Asia: A study by ultra-high-Resolution mass spectrometry, Environ. Sci. Technol., 46, 13118–13127, 2012.

Lopez-Hilfiker, F. D., Mohr, C., Ehn, M., Rubach, F., Kleist, E., Wildt, J., Mentel, Th. F., Lutz, A., Hallquist, M., Worsnop, D., and Thornton, J. A.: A novel method for online analysis of gas and particle composition: description and evaluation
10   of a Filter Inlet for Gases and AEROsols (FIGAERO), Atmos. Meas. Tech., 7, 983–1001, 2014.

Mohr, C., Lopez-Hilfiker, F. D., Zotter, P., Prévôt, A. S. H., Xu, L., Ng, N. L., Herndon, S. C., Williams, L. R., Franklin, J. P., Zahniser, M. S., Worsnop, D. R., Knighton, W. B., Aiken, A. C., Gorkowski, K. J., Dubey, M. K., Allan, J. D., and Thornton, J. A.: Contribution of nitrated phenols to wood burning brown carbon light absorption in Detling, United Kingdom during winter time, Environ. Sci. Technol., 47, 6316–6324, 2013.

15   Murphy, D. M., Cziczo, D. J., Hudson, P. K., and Thomson, D. S.: Carbonaceous material in aerosol particles in the lower stratosphere and tropopause region, J. Geophys. Res., 112, 2007.

Nozière, B., Ekstrom, S., Alsberg, T., and Holmstrom, S.: Radical-initiated formation of organosulfates and surfactants in atmospheric aerosols, Geophys. Res. Lett., 37, 2010.

Olson, C. N., Galloway, M. M., Yu, G., Hedman, C. J., Lockett, M. R., Yoon, T., Stone, E. A., Smith, L. M., and Keutsch,
20   F. N.: Hydroxycarboxylic acid-derived organosulfates: Synthesis, stability, and quantification in ambient aerosol, Environ. Sci. Technol., 45, 15, 6468–6474, 2011.

Pope, C. A., Burnett, R. T., Thun, M. J., Calle, E. E., Krewski, D., Ito, K., and Thurston, G. D.: Lung cancer, cardiopulmonary mortality, and long-term exposure to fine particulate air pollution, J. Am. Med. Assoc., 287(9), 1132–1141, 2002.

25   Reemtsma, T., Weiss, S., Mueller, J., Petrovic, M., Gonzalez, S., Barcelo, D., Ventura, F., and Knepper, T. P.: Polar pollutants entry into the water cycle by municipal wastewater: A European perspective, Environ. Sci. Tech. 40, 2006.

Riva, M., Tomaz, S., Cui, T., Lin, Y-H, Perraudin, E., Gold, A., Stone, E. A., Villenave, E., and Surratt, J. D.: Evidence for an unrecognized secondary anthropogenic source of organosulfates and sulfonates: gas-phase oxidation of polycyclic aromatic hydrocarbons in the presence of sulfate aerosol, Environ. Sci. Technol., 49 (11), 6654–6664, 2015.

30   Riva, M., Da Silva Barbosa, T., Lin, Y.-H., Stone, E. A., Gold, A., and Surratt, J. D.: Chemical characterization of organosulfates in secondary organic aerosol derived from the photooxidation of alkanes, Atmos. Chem. Phys., 16, 11001-11018, https://doi.org/10.5194/acp-16-11001-2016, 2016.

Schindelka, J., Iinuma, Y., Hoffmann, D., and Herrmann, H.: Sulfate radical-initiated formation of isoprene-derived organosulfates in atmospheric aerosols, Faraday Discuss., 165,237–259, 2013.

Shalamzari, M. S., Ryabtsova, O., Kahnt, A., Vermeylen, R., Herent, M. F., Quetin-Leclercq, J., Van der Veken, P., Maenhaut, W., and Claeys, M.: Mass spectrometric characterization of organosulfates related to secondary organic aerosol from isoprene, Rapid Commun. Mass Spectrom., 784–794, 2013.

Shalamzari, S. M., Ryabtsova, O., Kahnt, A., Vermeylen, R., Hérent, M.-F., Quetin-Leclercq, J., Van Der Veken, P., Maenhaut, W., and Claeys, M.: Mass spectrometric characterization of organosulfates related to secondary organic aerosol from isoprene, Rapid Commun. Mass Spectrom., 27, 784–794, 2013. Shalamzari, M. S., Kahnt, A., Vermeylen, R., Kleindiesnt, T. E., Lewandowski, M., Cuyckens, F., Maenhaut, W., and Claeys, M.: Characterization of polar organosulfates in secondary organic aerosol from the green leaf volatile 3-Z-hexenal, Environ. Sci. Technol., 48, 12671–12678, 2014.

Smith, J. N., Dunn, M. J., VanReken, T. M., Iida, K., Stolzenburg, M. R, McMurry, P. H., and Huey, L. G.: Chemical composition of atmospheric nanoparticles formed from nucleation in Tecamac, Mexico: Evidence for an important role for organic species in nanoparticle growth, Geophys. Res. Lett., 35, 4, 2008.

Stark, H., R. L. N. Yatavelli, S. L. Thompson, H. Kang, J. E. Krechmer, J. R. Kimmel, B. B. Palm, W. Hu, P. L. Hayes, D. A. Day, P. Campuzano-Jost, M. R. Canagaratna, J. T. Jayne, D. R. Worsnop, and J. L. Jimenez: Impact of Thermal Decomposition on Thermal Desorption Instruments: Advantage of Thermogram Analysis for Quantifying Volatility Distributions of Organic Species, Environ Sci Technol, doi:10.1021/acs.est.7b00160, 2017.

Staudt, S., Kundu, S., He, X., Lehmler, H. J., Lin, Y. H., Cui, T. Q., Kristensen, K., Glasius, M., Zhang, X., Weber, R., Surratt, J. D., and Stone, E. A.: Aromatic organosulfates in atmospheric aerosols: Synthesis, characterization, and abundance, Atmos. Environ., 94, 366–373, 2014.

Stone, E. A., Yang, L., Yu, L. E., and Rupakheti, M.: Characterization of organosulfates in atmospheric aerosols at Four Asian locations, Atmos. Environ., 47, 323–329, 2012.

Surratt, J. D., Lewandowski, M., Offenberg, J. H., Jaoui, M., Kleindiesnt, T. E., Edney, E. O., and Seinfeld, J. H.: Effect of acidity on secondary organic aerosol formation from isoprene, Environ. Sci. Technol., 41, 5363–5369, 2017.

Surratt, J. D., Gomez-Gonzalez, Y., Chan, A. W. H., Vermeylen, R., Shahgholi, M., Kleindiesnt, T. E., Edney, E. O., Offenberg, J. H., Lewandowski, M., Jaoui, M., Maenhaut, W., Claeys, M., Flagan, R. C., and Seinfeld, J. H.: Organic sulfate formation in biogenic secondary organic aerosol, J. Phys. Chem., 112, 8345– 8378, 2008.

Surratt, J. D., Chan, A. W. H., Eddingsaas, N. C., Chan, M. N., Loza, C. L., Kwan, A. J., Hersey, S. P., Flagan, R. C., Wennberg, P. O., and Seinfeld, J. H.: Reactive intermediates revealed in secondary organic aerosol formation from isoprene, Proc. Natl. Acad. Sci. U.S.A. 2010.

Wang, X. K., Rossignol, S., Ma, Y., Yao, L., Wang, M., Chen, J. M., George, C. and Wang, L.: Molecular characterization of atmospheric particulate organosulfates in three megacities at the middle and lower reaches of the Yangtze River, Atmos. Chem. Phys., 16, 2285-2298, 2016.

Worton, D. R., Surratt, J. D., Lafranchi, B. W., Chan, A. W., Zhao, Y., Weber, R. J., Park, J. H., Gilman, J. B., de Gouw, J., Park, C., Schade, G., Beaver, M., Clair, J. M., Crounse, J., Wennberg, P., Wolfe, G. M., Harrold, S., Thornton, J. A.,

Farmer, D. K., Docherty, K. S., Cubison, M. J., Jimenez, J. L., Frossard, A. A., Russell, L. M., Kristensen, K., Glasius, M., Mao, J., Ren, X., Brune, W., Browne, E. C., Pusede, S. E., Cohen, R. C., Seinfeld, J. H., and Goldstein, A. H.: Observational insights into aerosol formation from isoprene, Environ. Sci. Technol., 47, 11403–11413, 2013.

Wuebbles, D. J. and Jain, A. K.: Concerns about climate change and the role of fossil fuel use, Fuel. Process. Techn., 71, 99-119, 2001.

Zhang, H., Worton, D. R., Lewandowski, M., Ortega, J., Rubitschun, C. L., Park, J.-H., Kristensen, K., Campuzano-Jost, P., Day, D. A., Jimenez, J. L., Jaoui, M., Offenberg, J. H., Kleindienst, T. E., Gilman, J., Kuster, W. C., de Gouw, J., Park, C., Schade, G. W., Frossard, A. A., Russell, L., Kaser, L., Jud, W., Hansel, A., Cappellin, L., Karl, T., Glasius, M., Guenther, A., Goldstein, A. H., Seinfeld, J. H., Gold, A., Kamens, R. M., and Surratt, J. D.: Organosulfates as tracers for secondary organic aerosol (SOA) formation from 2-methyl-3-buten-2-ol (MBO) in the atmosphere, Environ. Sci. Technol., 46, 9437–9446, 2012b.

Zhang, Q., He, K., and Huo, H.: Policy: Cleaning China's air, Nature, 484, 161–162, 2012a.

Zhang, Q., Jimenez, J. L., Worsnop, D. R., and Canagaratna, M.: A case study of urban particle acidity and its influence on secondary organic aerosol, Environ. Sci. Technol. 2007.
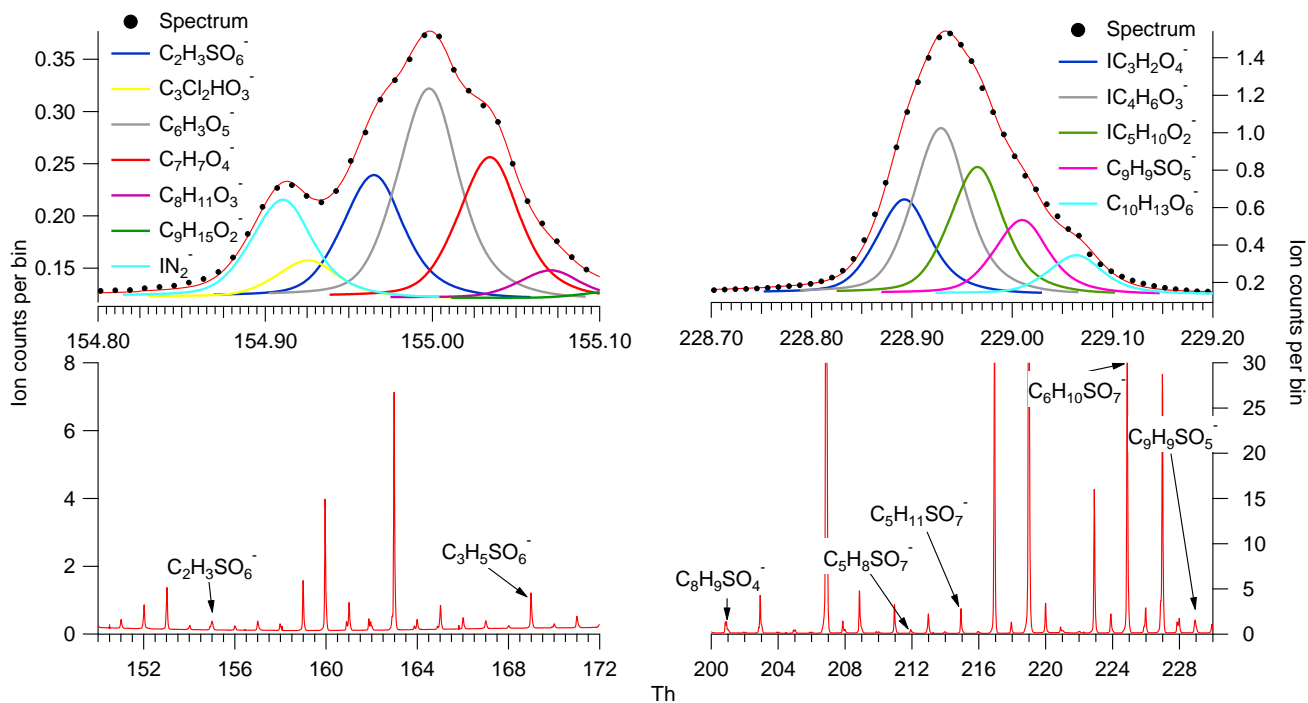
Figure 1. The bottom panel displays the average campaign mass spectrum for the whole mass range of the ToF (3-620) which is further expanded to show small regions in the middle panel and specific and HR fitting for individual peaks in the top panel.

Table 1. SCOs identified at the Changping site with their respective mass, chemical name and potential precursors.

m/z ion	Molecular formula	Reference	OS name	Precursor	[mean] µgm-3	mean % PM	mean % OA	mean % OS
154.965582	$C_2H_3SO_6^-$	Surrat 2007	Glycolic acid sulphate	Glycolic acid	2.97	0.02	0.03	1.6
168.981232	$C_3H_5SO_6^-$	Olson 2011	Lactic acid sulphate	Lactic acid	13.00	0.07	0.14	5.9
171.012139	$C_7H_7SO_3^-$	Riva 2015		Aromatics (Benzene and PAHs)	6.00	0.03	0.06	2.7
172.019964	$C_7H_8SO_3^-$	Riva 2015		Aromatics (Benzene and PAHs)	4.00	0.02	0.04	0.9
184.991403	$C_7H_5SO_4^-$	Riva 2015		Aromatics (Benzene and PAHs)	24.00	0.12	0.25	12.1
187.007053	$C_7H_7SO_4^-$	Staudt 2014	Methyl phenyl sulphate	benzene	14.00	0.07	0.15	6.7
199.007053	$C_8H_7SO_4^-$	Riva 2015		Aromatics (Benzene and PAHs)	5.00	0.03	0.05	2.4
199.999622	$C_4H_8SO_7^-$	Surrat 2007		2-methylglyceric acid (isoprene)	3.00	0.02	0.03	0.8
201.022703	$C_8H_9SO_4^-$	Staudt 2014	4 methyl benzyl sulphate	benzene	6.00	0.03	0.06	3.7
211.999622	$C_5H_8SO_7^-$	Surrat 2008		isoprene	2.00	0.01	0.02	1.3
215.023097	$C_5H_{11}SO_7^-$	Surrat 2010	IEPOX sulphate	IEPOX	11.00	0.06	0.12	4.5
217.9759	$C_6H_4NSO_6^-$	-	Nitrophenol sulphate	Nitrophenol	1.00	0.01	0.01	0.4
226.015272	$C_6H_{10}SO_7^-$	Boris 2016	unknown	unknown	30.00	0.16	0.32	15.1
229.017618	$C_9H_9SO_5^-$	Riva 2015		Aromatics (Benzene and PAHs)	10.00	0.05	0.11	5.0
231.033268	$C_9H_{11}SO_5^-$	Riva 2015		Aromatics (Benzene and PAHs)	13.00	0.07	0.14	6.7
287.023097	$C_{11}H_{11}SO_7^-$	Riva 2015		Aromatics (Benzene and PAHs)	40.00	0.21	0.42	20.2
294.065296	$C_{10}H_{16}NSO_7^-$	Surrat 2008		alpha pinene	21.00	0.00	0.22	9.9
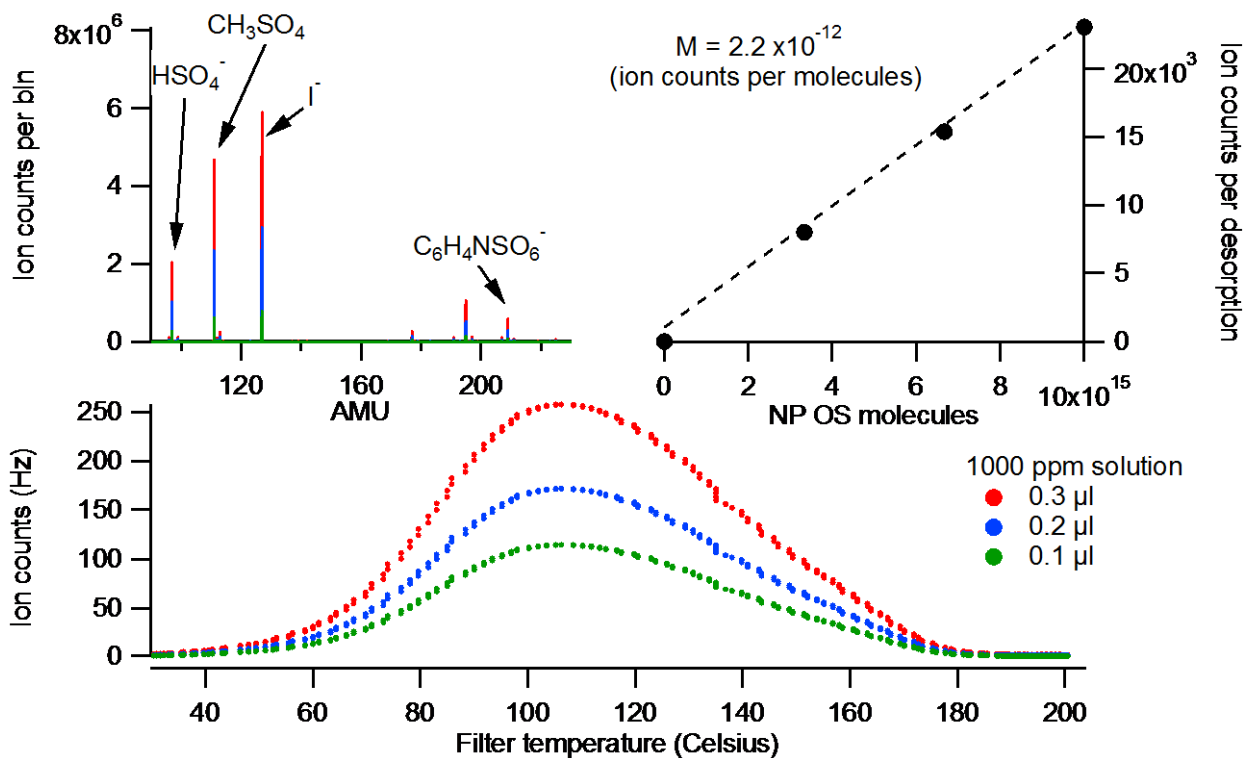
Figure 2. The desorption profile of NP OS 3 step calibrations for 0.1 μl, 0.2 μl and 0.3 μl 1000 ppm solution is displayed in the bottom panel and its corresponding average stick spectra (top left) and sum of counts per molecule loading for each calibration (top right)
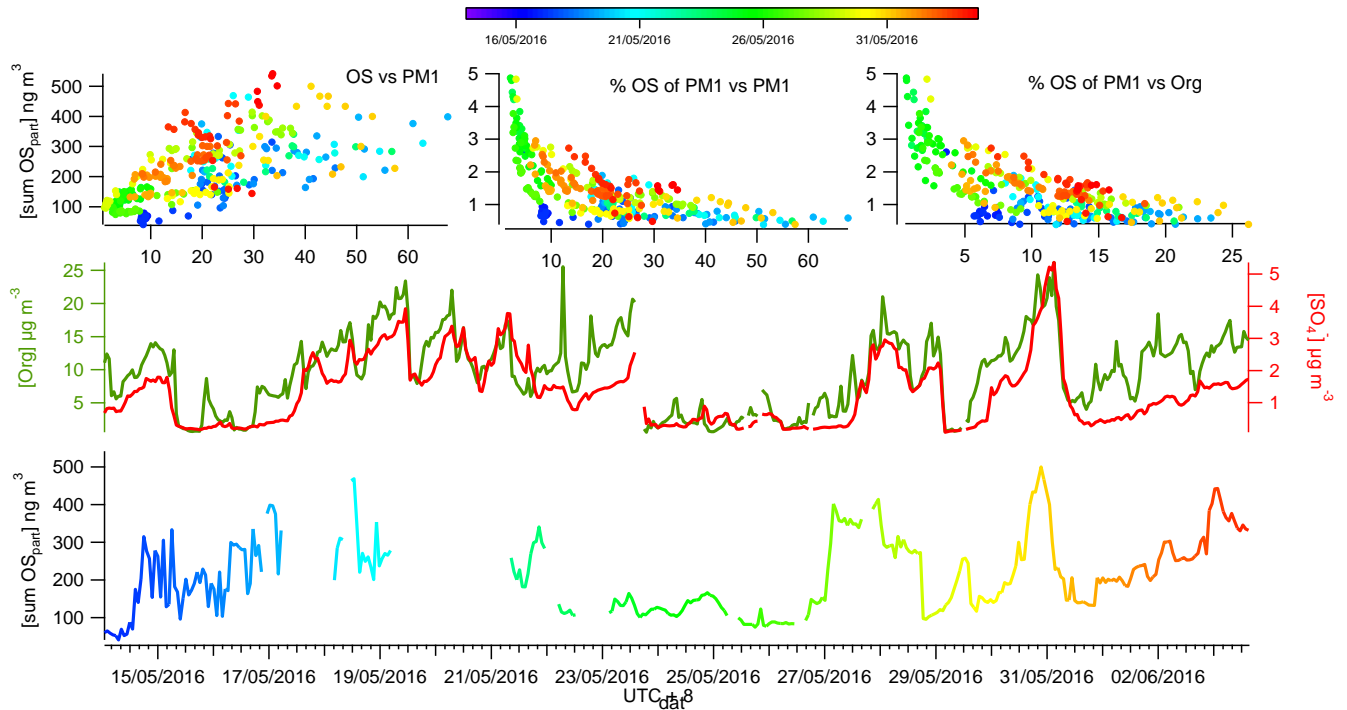
Figure 3. Time series of total SCO (colour coded with time) is displayed in the bottom panel. The time series of the AMS organic (green) and sulfate (red) is displayed in the middle panel and the correlation of SCO to PM₁, mass fraction of PM₁ and organics are displayed in the upper panel. The colour coding represents time throughout the campaign.
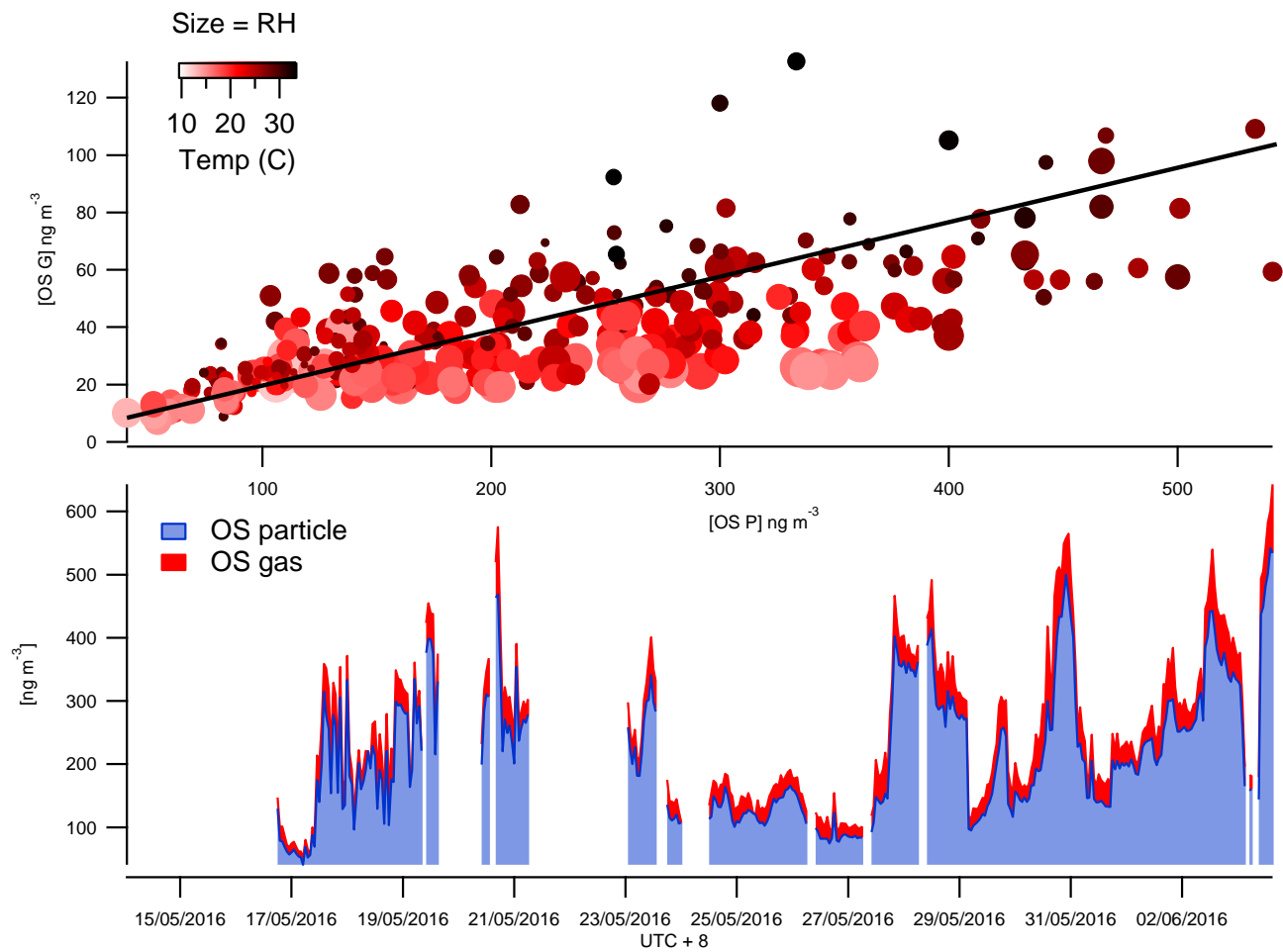
Figure 4. Time series of total SCOs in the gas and particle phase (bottom panel) and their correlation colour coded by temperature and size binned by relative humidity (top panel).
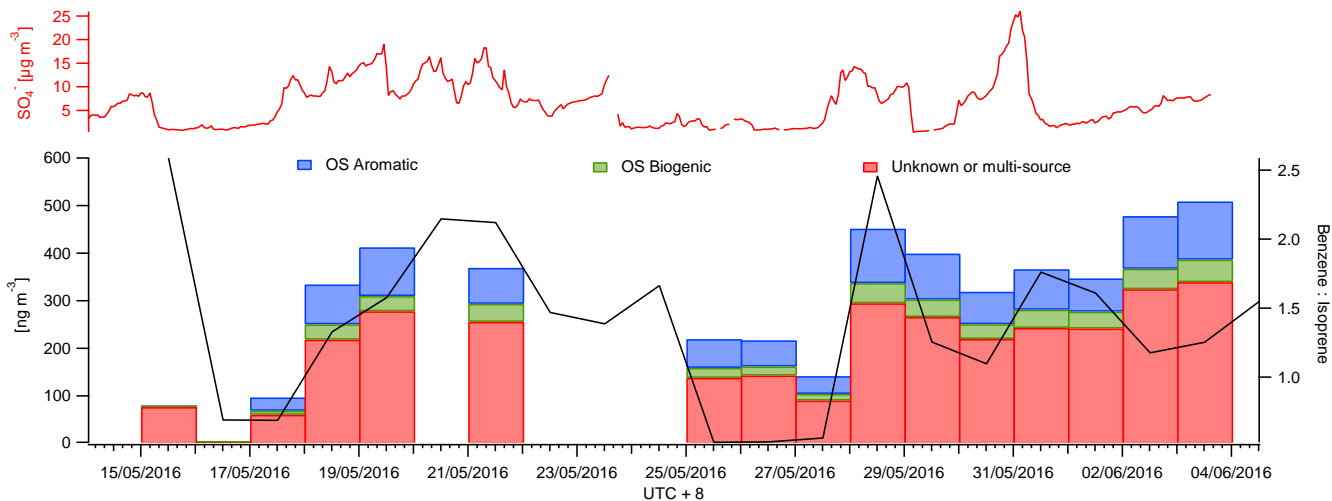
Figure 5. A time series of the mean daily benzene to isoprene ratio as a marker for anthropogenic and biogenic influence (black) is displayed in the top panel. The CIMS data was also binned to provide mean daily SCO concentrations for aromatic (blue) and biogenic (green) precursor SCOs (bottom panel). The red bars represent SCOs with an unknown source or SCO produced via both biogenic and anthropogenic pathways. The AMS SO$_4^{2-}$ concentration is also presented to indicate availability of sulfur in the particle phase.
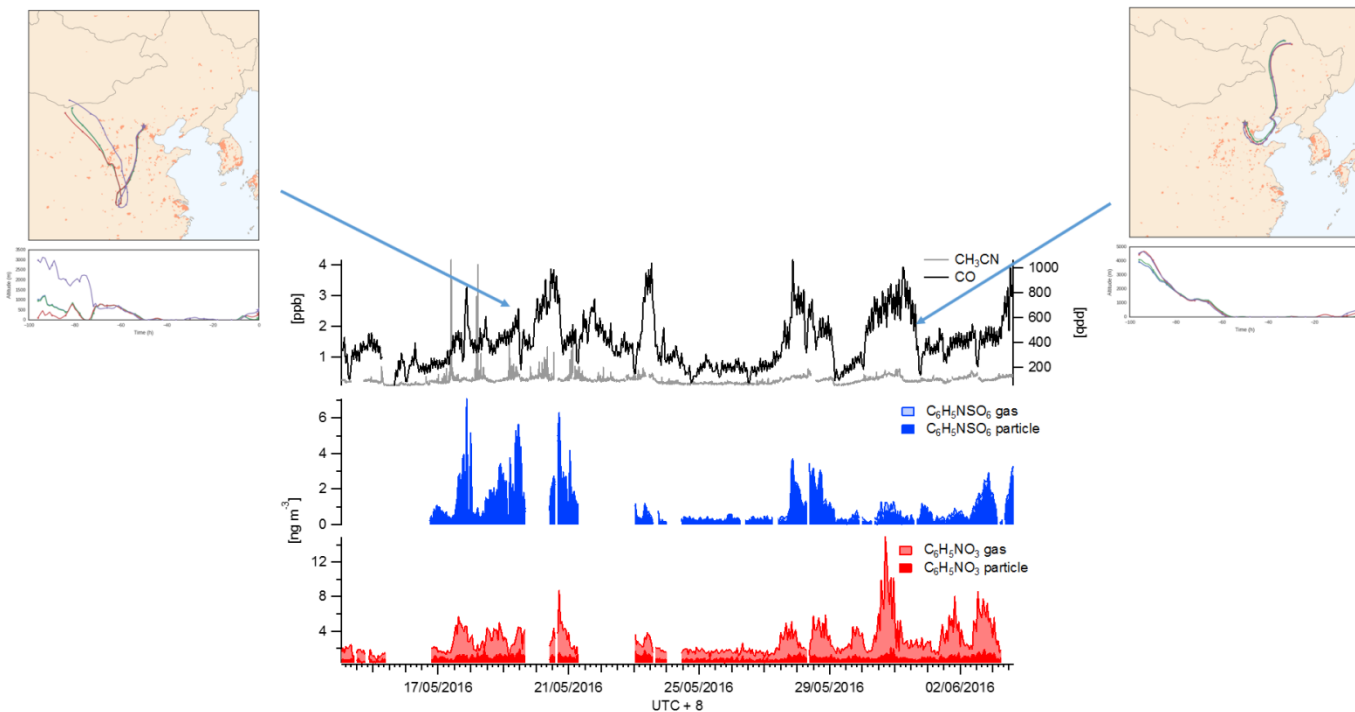
Figure 6. Time series of gas and particle phase NP (red), NP OS (blue) and gas phase acetonitrile (grey) and CO (black) between the 16th and 3rd June
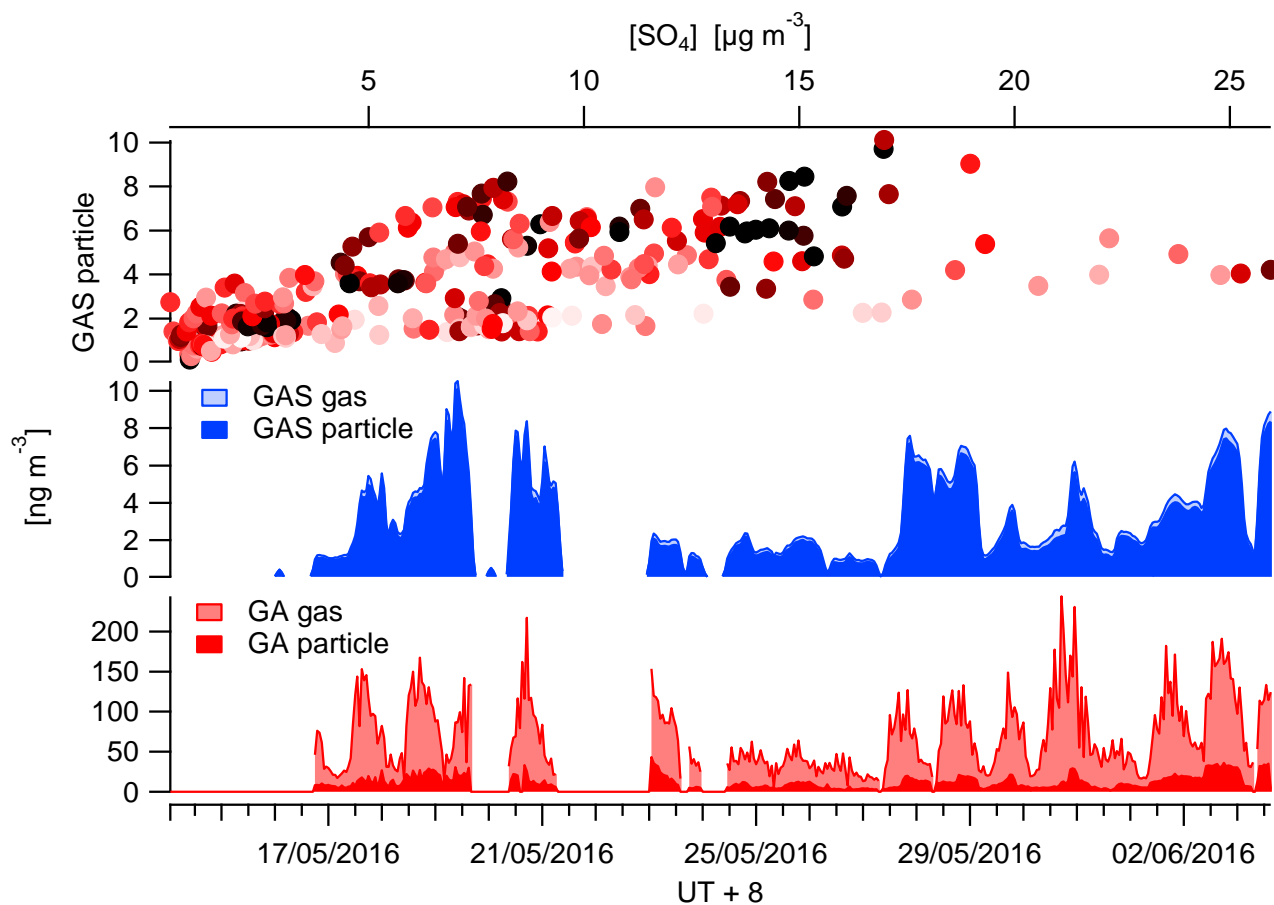
Figure 7. Campaign time series of glycolic acid (red) and GAS (blue) in the particle and gas phase. The top panel illustrates the correlation between GAS in the particle phase and SO_4^{2-} colour coded by GAp/GAg.

(A)

(B)
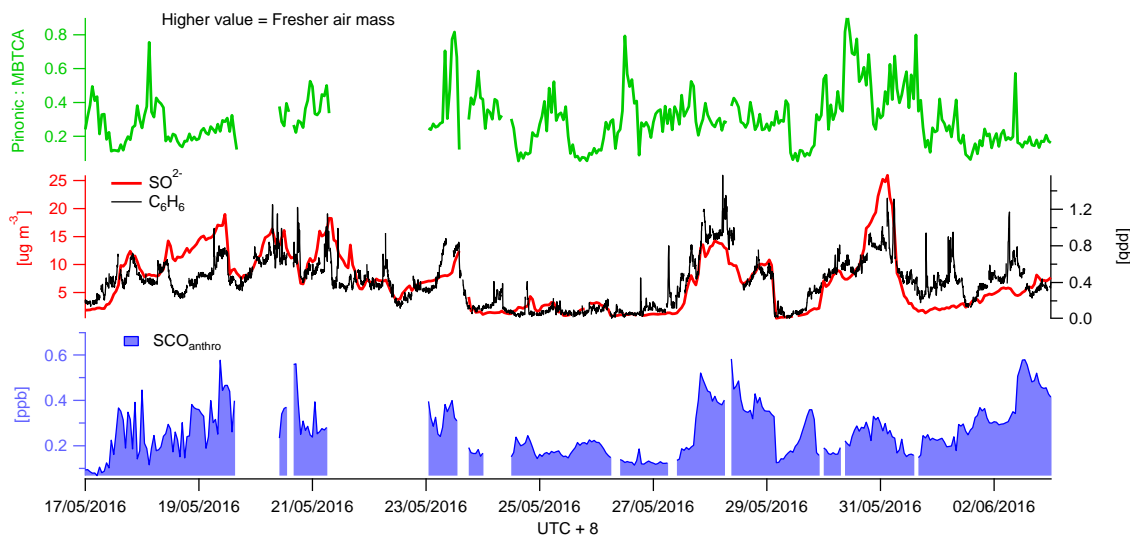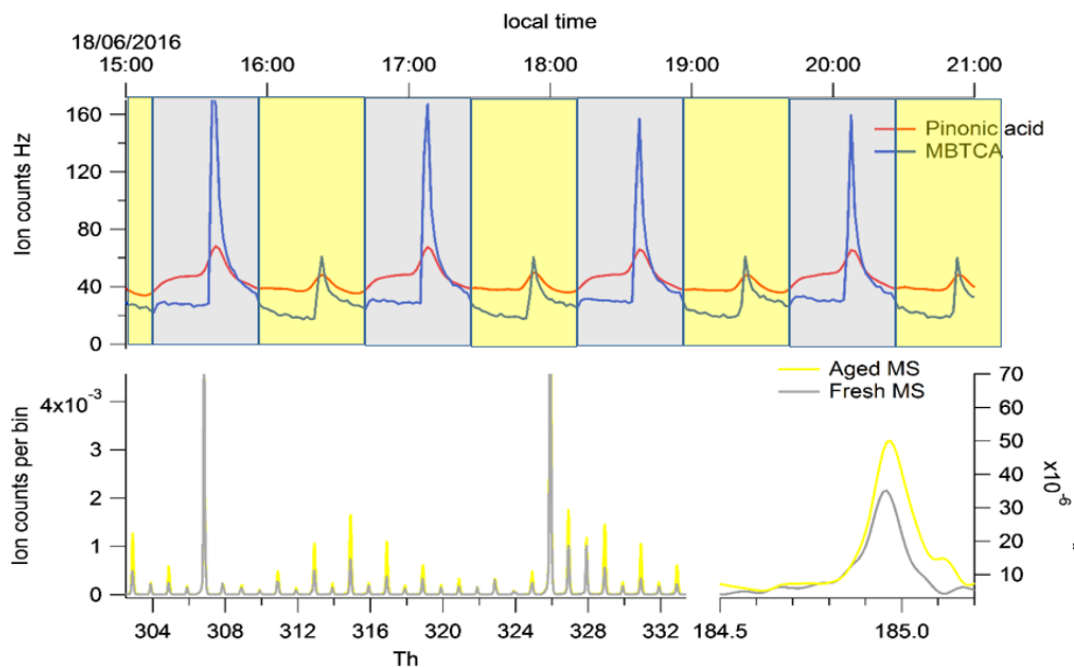
Figure 8. (A) Total benzene/PAH derived SCO (SCO$_{anthro}$) time series and respective SO$_4^{2-}$ and benzene concentrations. The indicator of photochemical aging (pinonic acid: MBTCA) is plotted in green. (B) illustrates the mass spectral difference between fresh and aged air masses through Go:PAM and respective time series for pinonic acid and MBTCA.
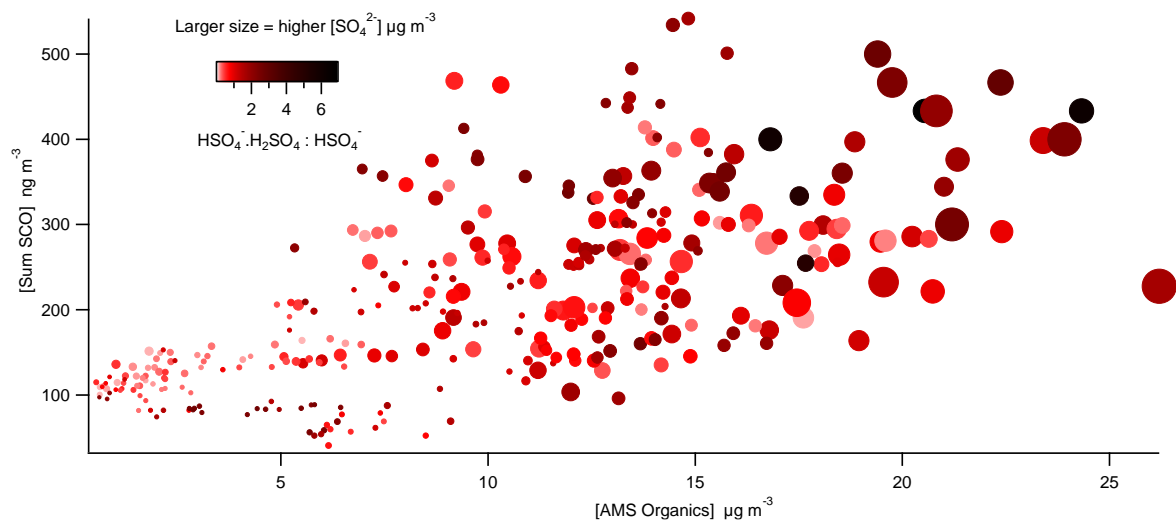
Figure 9. Correlation plot of total SCOs vs total particle phase organics as a function of acidity (colour coding counts of HSO₄⁻.H₂SO₄: HSO₄) and SO₄²⁻ (data point size spanning concentrations from 0.2 to 16 µg m⁻³).